Acta Crystallographica Section A
Foundations of Crystallography
ISSN 0108-7673

Received 27 May 2008
Accepted 7 August 2008

Computing with almost periodic functions

R. V. Moody,[a]* M. Nesterenko[b] and J. Patera[c]

[a]Department of Mathematics, University of Victoria, British Columbia, Canada, [b]Institute of Mathematics, NAS of Ukraine, 3 Tereshchenkivs'ka Street, Kyiv, 01601, Ukraine, and [c]Centre de Recherches Mathématiques, Université de Montréal, CP 6128–Centre ville, Montréal, Québec, Canada H3C 3J7. Correspondence e-mail: rmoody@uvic.ca

This paper develops a method for discrete computational Fourier analysis of functions defined on quasicrystals and other almost periodic sets. A key point is to build the analysis around the emerging theory of quasicrystals and diffraction in the setting on local hulls and dynamical systems. Numerically computed approximations arising in this way are built out of the Fourier module of the quasicrystal in question and approximate their target functions uniformly on the entire infinite space. The methods are entirely group theoretical, being based on finite groups and their duals, and they are practical and computable. Examples of functions based on the standard Fibonacci quasicrystal serve to illustrate the method (which is applicable to all quasicrystals modeled on the cut-and-project formalism).

1. Introduction

In this paper we consider the problem of discrete methods for dealing with functions that are intrinsically almost periodic, but not actually periodic. Quasicrystals, quasicrystalline photonic crystals, Faraday-wave experiments and other physical phenomena arising from the interaction of incommensurate frequencies all display the features of almost periodicity. As a typical example one may think of a potential field of a physical quasicrystal. The salient features of quasicrystals are highly structured long-range order (represented by pure point or near pure point diffraction) but no periodic order. Thus the potential is not a periodic function, but rather belongs to the domain of almost periodic functions.

Here we put forth a method for finite discrete analysis of almost periodic functions that has the following main features:

(1) It is entirely based on group-theoretical methods, primarily finite groups and their duals.

(2) The discretely computed Fourier approximants are themselves almost periodic and uniformly approximate their target functions over their entire domains.

(3) The Fourier frequencies involved in the approximation lie in the module of Fourier frequencies of the target function.

A standard approach to modeling such a structure is to take a finite part of it, impose periodic boundary conditions, rationalize and reduce the object to a periodic approximant, and then apply usual crystallography. Although this type of periodization is used routinely and successfully for many modeling problems in the theory of quasicrystals, it is not entirely satisfactory. Almost periodic order goes beyond periodic order in fundamental ways, its essence appearing as an underlying incommensurability which pervades every part of the theory. For instance, a key feature of quasicrystals appears in the Fourier module that parameterizes the Bragg spectrum and always has rank higher than (typically double) the dimension of the ambient space of the quasicrystal. Periodization destroys this and by its nature can only produce results that can fit data over the finite range specified by the imposed periodization boundaries, whereas the essence of the material is that its order is long range. The present paper does not involve any periodization and avoids these issues.

The theory of almost periodic functions was initiated by Bohr (1947), on the basis of earlier work on uniform approximation of functions by trigonometric polynomials by Bohl (1893). It was greatly extended by the work of Besicovitch (1954), Bochner (1927, 1962), Bochner & von Neumann (1935), Wiener (1926), Weyl (1926–1927) and others (Burckel, 1970; Levitan & Zhikov, 1982; Amerio & Prouse, 1971). The advent of quasicrystals and aperiodic tilings instigated a revival of the field and led to extensive study of the cut-and-project formalism and the theory of pure point diffraction (Meyer, 1972; Moody, 1997; Hof, 1995; Schlottmann, 2000), which have become the mainstays of experimentalists and theorists alike. An important component of this is the use of dynamical systems and dynamical hulls. These are ideally suited to the phenomenon of almost periodicity, which appears in the dynamics as recurrence, and provide a natural setting for the Fourier analysis used in its study.

Although our study is of almost periodic functions, their importance in the subject of quasicrystals is that they arise from functions whose behavior is dominated by the local environment of the quasicrystal in question. The way in which this happens is mostly taken for granted, but in fact there are some interesting assumptions involved, and for this reason we begin by formally defining local functions with respect to a

given point set Λ in some real space $\mathbb{R}^d$ and showing how it is that they are connected with almost periodic functions.

We can create a *dynamical hull* (X, μ) from Λ. This is a compact space that arises from Λ and its translations, and it lies at the heart of the Fourier analysis of local functions on Λ. One assumes (in many important cases it is forced) a probability measure μ on which $\mathbb{R}^d$ acts in a measure-preserving way. A local function f lifts to some new function F on (X, μ), and this is an L^2 function. Now the analysis of f can be related directly to the analysis of F, and for this we have a powerful tool in the form of the action of $\mathbb{R}^d$ on $L^2(X, \mu)$, which is unitary. All of this material is explained in §2.

To go further, we next place ourselves in the situation of the cut-and-project formalism, which is the standard method of modeling used in the study of quasicrystals. The set Λ is now assumed to be a model set (cut-and-project set). In this setting the hull (X, μ), and more particularly $L^2(X, \mu)$, can be described explicitly in terms of a higher-dimensional torus[1] (higher-dimensional periodicity!), and it is a straightforward matter to carry out Fourier analysis of F. It is the restriction of this Fourier analysis back to f that provides the required Fourier analysis of f. By its very nature this is almost periodic and captures the full aperiodic nature of Λ, including the correct Fourier module in which physical information actually appears. This is the content of §3. Readers familiar with the cut-and-project method who do not wish to go through the theory of local hulls and local functions may read §§3.1 and 3.4, and then move on to §4.

This theoretical analysis is based on higher-dimensional structures that are not explicitly computable, as well as the usual array of countably many Fourier coefficients, each of which is the outcome of integration. To be a practical tool, the analysis has to be reduced to finitely many objects that are explicitly computable entirely in the context of the given function f. The resulting approximants are trigonometric polynomials (quasi-periodic functions) whose frequencies come from the Fourier module of the original function. In §4 we outline the method of discretization, which depends primarily on the construction of a refinement lattice of the lattice of the cut-and-project scheme and, along with it, its dual lattice. Together these produce two finite groups which are in $\mathbb{Z}$-duality to each other. The selection of data points and appropriate Fourier frequencies is governed by these two groups.

This analysis is best illustrated by examples, and for this purpose we have chosen two local functions based on one of the famous Fibonacci point sets. This has the advantage of being straightforward to construct and easy to visualize, while at the same time containing all the essential features of more general model sets. §5 prepares the mathematics of the Fibonacci cut-and-project scheme, and §6 shows some explicit computations for the particular local functions we have chosen. As is evident from the examples, the main effort required is in the creation of the data points. Once this is done, the same set of data points and Fourier frequencies will work for any almost periodic function arising from the same cut-and-project scheme.

The results are striking in two ways. First of all, the approximating functions are remarkably good, given the amount of data from which they are produced. Secondly, the approximating functions are not just local approximations, they are also *global* approximations, in the sense that they provide finite Fourier series that approximate f throughout its entire domain. Of course this was to be expected, but it is impressive to see it in action.

The numerical methods we introduce here are designed to be efficient and, of course, to utilize the inherent almost periodicity. In the development of the theory we provide error estimates that can be worked out specifically in the cases of interest. We note that the primary weakness in the error estimates is not one that is due to the aperiodic nature of the problem but one that always appears in Fourier analysis, namely how well can one approximate a function if one uses only finitely many of its Fourier coefficients.

2. Continuous functions on aperiodic point sets

2.1. Local hulls

For $r > 0$, let $D_r(\mathbb{R}^d)$ be all point sets $\Lambda \subset \mathbb{R}^d$ for which the distance $|x - y| \geq r$ for all $x, y \in \Lambda$. This means that D_r consists of all discrete point sets with minimal separation $\geq r$ between their points.

The *local topology* on $D_r(\mathbb{R}^d)$ can be intuitively introduced as follows. Two sets Λ_1 and Λ_2 of $D_r(\mathbb{R}^d)$ are 'close' if, for some large R and some small ϵ, one has

$$\begin{aligned} \Lambda_1 \cap B_R &\subset \Lambda_2 + B_\epsilon, \\ \Lambda_2 \cap B_R &\subset \Lambda_1 + B_\epsilon, \end{aligned} \tag{1}$$

where B_R (B_ϵ) is ball of radius R (ϵ) around 0. Thus for each point of Λ_1 within the ball B_R, there is a point of Λ_2 within a distance ϵ of that point, and *vice versa*. Pairs (Λ_1, Λ_2) satisfying equation (1) are called (R, ϵ)-close (Fig. 1).

The local topology is actually a metric topology, although we make no use of this fact here.

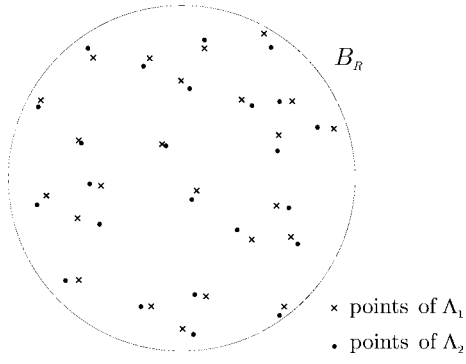

Figure 1
Two sets Λ_1 and Λ_2 of $D_r(\mathbb{R}^d)$ that are close.

[1] More generally a compact Abelian group.

Definition 1. For $\Lambda \in D_r(\mathbb{R}^d)$ the local hull of Λ is

$$X(\Lambda) = \overline{\{t + \Lambda : t \in \mathbb{R}^d\}} \subset D_r(\mathbb{R}^d), \tag{2}$$

i.e. take all translates of Λ and take their closure in the local topology.

Proposition 2.1 (Radin & Wolf, 1992). The translation action of $\mathbb{R}^d$ on Λ lifts to a translation action on $X(\Lambda)$. The local hull $X(\Lambda)$ is compact and the $\mathbb{R}^d$-action on it is continuous.

Example 1. Let Λ be the lattice $\mathbb{Z}^d$ in $\mathbb{R}^d$. Then $X(\Lambda) = \mathbb{R}^d/\mathbb{Z}^d$ is the d-torus (with its usual topology). Intuitively we translate the lattice around with $\mathbb{R}^d$. However, translation by an element of $\mathbb{Z}^d$ leaves Λ invariant, so $\mathbb{R}^d/\mathbb{Z}^d$ parameterizes all distinct positions of Λ under translation.

Example 2. Let Λ be any Penrose tiling. Then $X(\Lambda)$ is the set of all Penrose tilings that are locally indistinguishable from some translate of Λ. $X(\Lambda)$ contains considerably more than just the translations of Λ. In fact $X(\Lambda)$ consists of all Penrose tilings based on the same pair of Penrose rhombs and the same orientations as appear in Λ.

Generally one may think of $X(\Lambda)$ as some sort of local indistinguishability class of Λ.

2.2. Continuous functions on $X(\Lambda)$

We assume that $\Lambda \subset D_r(\mathbb{R}^d)$ and $X(\Lambda)$ are as in §2.1.

Consider a function

$$F : X(\Lambda) \longrightarrow \mathbb{C}. \tag{3}$$

We can define from it a function

$$f : \mathbb{R}^d \longrightarrow \mathbb{C}$$

by

$$f(t) = F(t + \Lambda). \tag{4}$$

If F is continuous then we note that for all $t_1, t_2 \in \mathbb{R}^d$

$$\begin{aligned} & t_1 + \Lambda, t_2 + \Lambda \text{ are close} \\ \Longrightarrow \quad & F(t_1 + \Lambda), F(t_2 + \Lambda) \text{ are close} \\ \Longrightarrow \quad & f(t_1), f(t_2) \text{ are close.} \end{aligned}$$

Thus continuity of F implies continuity of f, and we see that f is local, or almost periodic, with respect to Λ in the following sense:

Definition 2. A function $f : \mathbb{R}^d \longrightarrow \mathbb{C}$ is called local with respect to a set $\Lambda \in D_r(\mathbb{R}^d)$, or Λ-local, if for all $\epsilon' > 0$ there exist R and ϵ so that whenever $t_1, t_2 \in \mathbb{R}^d$ satisfy that $t_1 + \Lambda$ and $t_2 + \Lambda$ are (R, ϵ)-close then

$$|f(t_1) - f(t_2)| < \epsilon'.$$

The intuitive meaning of this is that f has the very natural property, at least from the perspective of physical systems, that it looks very much the same at places where the local environment looks the same. Local functions are easily seen to be continuous on $\mathbb{R}^d$.

Using locality, we can go in the opposite direction. Let $\Lambda \in D_r(\mathbb{R}^d)$ and let $f : \mathbb{R}^d \to \mathbb{C}$ be local with respect to Λ. Define

$$F : \{t + \Lambda : t \in \mathbb{R}^d\} \longrightarrow \mathbb{C}$$

[so that F is a function on a part of $D_r(\mathbb{R}^d)$] by

$$F(t + \Lambda) = f(t).$$

Then F is continuous on $\{t + \Lambda : t \in \mathbb{R}^d\}$ with respect to the local topology. In fact it is *uniformly* continuous. The reason for this is that the continuity condition which defines the locality of f is based on the uniformity [*i.e.* the notion of (R, ϵ)-closeness] defining the local topology of $\{t + \Lambda : t \in \mathbb{R}^d\}$.

It follows that F lifts uniquely to a continuous function [equation (3)] on the local hull $X(\Lambda)$.

Proposition 2.2. For each local function f with respect to Λ there is a unique continuous function [equation (3)] on the local hull, whose restriction to the orbit of Λ is f. Every continuous function on the local hull of Λ arises in this way.

Thus we see that a locality with respect to Λ and the existence and continuity of an extension function on $X(\Lambda)$ amount to the same thing.

In the situation that $X(\Lambda)$ is equipped with an $\mathbb{R}^d$-invariant probability measure μ [*i.e.* a positive Borel measure μ with $\mu(t + A) = \mu(A)$ for all Borel sets and with $\mu\big(X(\Lambda)\big) = 1$], the action of $\mathbb{R}^d$ on $X(\Lambda)$ leads to unitary action T of $\mathbb{R}^d$ on $L^2\big(X(\Lambda), \mu\big)$. Namely for all $F \in L^2\big(X(\Lambda), \mu\big)$ and for all $t \in \mathbb{R}^d$, $T_t F$ is the function defined by $T_t F(\Gamma) = F(-t + \Gamma)$, and with

$$\langle F \mid G \rangle := \int_{X(\Lambda)} F\overline{G}\, \mathrm{d}\mu$$

we have

$$\langle T_t F \mid T_t G \rangle = \langle F \mid G \rangle.$$

In principle the spectral theory of $L^2\big(X(\Lambda), \mu\big)$ should allow one to analyze Λ-local functions $f : \mathbb{R}^d \to \mathbb{C}$ by analyzing their corresponding functions F on $L^2\big(X(\Lambda), \mu\big)$.

For one very important class of subsets Λ this can actually be carried out in detail – namely the class of model sets, which we now introduce.

3. Local functions on model sets

3.1. Cut-and-project schemes, model sets and torus parameterization

An important class of point sets $\Lambda \subset \mathbb{R}^d$ for which we know a considerable amount about the corresponding hulls $X(\Lambda)$ is the class of cut-and-project sets, or the model sets as they are often called (Meyer, 1972; Moody, 1997).

Consider the cut-and-project scheme

$$\begin{array}{ccccc} \mathbb{R}^d & \xleftarrow{\ \|\ } & \mathbb{R}^d \times \mathbb{R}^d & \xrightarrow{\ \perp\ } & \mathbb{R}^d \\ & & \cup & & \\ & \xleftarrow{\ 1\text{–}1\ } & \widetilde{L} & \xrightarrow{\ \text{dense image}\ } & \end{array} \tag{5}$$

and a window Ω. Here $\widetilde{L}$ is a lattice in $\mathbb{R}^d \times \mathbb{R}^d$ which is oriented so that the projections into $\mathbb{R}^d$ are 1–1 and dense, respectively.

In equation (5) the left-hand $\mathbb{R}^d$ is *physical space*, the space in which Λ is going to lie. The right-hand $\mathbb{R}^d$ is *internal space*, the one that will be used to control the projection of the lattice $\widetilde{L}$ into physical space. The image of $\widetilde{L}$ under projection into physical space is denoted by L. Since this projection is 1–1, $L \simeq \widetilde{L}$ as groups, so L is a free Abelian group of rank $2d$, *i.e.* it has a $\mathbb{Z}$-basis of $2d$ elements. However, it necessarily has accumulation points, and the typical situation is that L is dense in physical space.

It is convenient to use notation like $\tilde{x}, x, x'$ for the elements of $\widetilde{L}$ and their respective left and right projections. Then $\tilde{x} = (x, x')$ where x runs through L. This implies the existence of the mapping $(\cdot)' : L \to L'$ defined by $x \mapsto x'$, which passes from physical to internal space.

Note that this mapping $(\cdot)'$, as given, is only defined on L. It cannot be extended in any canonical way to a mapping $\mathbb{R}^d \to \mathbb{R}^d$. However it does extend canonically to the rational spans of the objects in question, and we shall make use of this later.

We choose a subset Ω in internal space. This *window* is assumed to be compact, to be equal to the closure of its interior and to have a boundary of measure 0. Using it we define

$$\Lambda = \Lambda(\Omega) = \{x : \tilde{x} \in \widetilde{L},\ x' \in \Omega\}. \tag{6}$$

Sets of the form $t + \Lambda(\Omega)$, $t \in \mathbb{R}^d$, are called *cut-and-project sets* or *model sets*.[2] In particular, for each $(x, y) \in \mathbb{R}^d \times \mathbb{R}^d$ we may define

$$\Lambda_{(x,y)} = x + \Lambda(-y + \Omega). \tag{7}$$

If $(x, y) \equiv (x', y') \bmod \widetilde{L}$, then $x + \Lambda(-y + \Omega) = x' + \Lambda(-y' + \Omega)$, as can be verified directly from the definitions. Thus these model sets are parameterized by the torus of dimension $2d$,

$$(\mathbb{R}^d \times \mathbb{R}^d)/\widetilde{L} \simeq (\mathbb{R}/\mathbb{Z})^d =: \mathbb{T}. \tag{8}$$

We note, though, that the parameterization need not necessarily be 1–1, *i.e.* in general, $\Lambda_{(x,y)} = \Lambda_{(x',y')} \not\Rightarrow (x, y) = (x', y') \bmod \widetilde{L}$. For simplicity, we shall usually write $(x, y)_L$ for the congruence class $(x, y) \bmod \widetilde{L}$.

There is a natural measure, the Haar measure, $\theta_{\mathbb{T}}$ on $\mathbb{T}$. This measure is the obvious 'area' measure in the case of $\mathbb{T}^2$ and 'length' measure for $\mathbb{T}^1$. It is invariant under the $\mathbb{R}^d$-action: $\mathbb{R}^d$ acts on $\mathbb{R}^{2d}/\widetilde{L}$ by

$$t + (x, y)_L = (t + x, y)_L. \tag{9}$$

Of particular importance to us is natural embedding (see Fig. 2),

$$\mathbb{R}^d \longrightarrow \mathbb{T}, \quad t \mapsto (t, 0)_L, \tag{10}$$

which lies behind the connection between almost periodicity in physical space and periodicity in some higher-dimensional setting. The image of this mapping is easily established to be dense in $\mathbb{T}$.

Now start with $\Lambda = \Lambda_{(0,0)} = \Lambda(\Omega)$ and translate it by elements $t \in \mathbb{R}^d$:

$$t + \Lambda(\Omega) = t + \Lambda(0 + \Omega) = \Lambda_{(t,0)}. \tag{11}$$

Then form the local hull $X(\Lambda)$, the closure of the set of all translates $\Lambda_{(t,0)}$ of Λ under the local topology [equation (2)].

Proposition 3.1 (Schlottmann, 2000). There is a continuous mapping,

$$\beta : X(\Lambda) \longrightarrow \mathbb{T}, \tag{12}$$

called the torus parameterization, such that

(1) β is onto;

(2) β is 1–1 almost everywhere, seen from the perspective of the Haar measure on $\mathbb{T}$;

(3) for all $t \in \mathbb{R}^d$, for all $\Lambda' \in X(\Lambda)$, one has $\beta(t + \Lambda') = t + \beta(\Lambda')$;

(4) $\beta(t + \Lambda) = (t, 0)_L$ for all $t \in \mathbb{R}^d$.

$X(\Lambda)$ and $\mathbb{T}$ are both compact spaces with natural $\mathbb{R}^d$-action, and $\beta : X(\Lambda) \to \mathbb{T}$ is an onto $\mathbb{R}^d$ mapping. However, $X(\Lambda)$ and $\mathbb{T}$ are subtly different. Although $t + \Lambda \in X(\Lambda)$ and $t + \Lambda \mapsto \Lambda_{(t,0)}$ for all t, not every element of $X(\Lambda)$ is a $\Lambda_{(x,y)}$ for some (x, y). Rather, when $(-y + \partial\Omega) \cap L' \neq \emptyset$ then for all $x \in \mathbb{R}^d$ there are always $\Lambda_1 \neq \Lambda_2$ elements of $X(\Lambda)$ that are mapped by β to the same $(x, y)_L$. When $\widetilde{z} = (z, z') \in \widetilde{L}$ with $z' \in (-y + \partial\Omega)$ then there will always be $\Lambda_1, \Lambda_2 \in X(\Lambda)$ with $\beta\big(X(\Lambda_1)\big) = \beta\big(X(\Lambda_2)\big) = (x, y)_L$, yet $x + z \in \Lambda_1$, $x + z \notin \Lambda_2$. In other words, there are ambiguities regarding the lattice points that project onto the boundary $\partial\Omega$ of Ω. An example of this is shown in the footnote appearing in §5.3. The fact that β is 1–1 almost everywhere arises from our assumption that the boundary of Ω has measure 0.

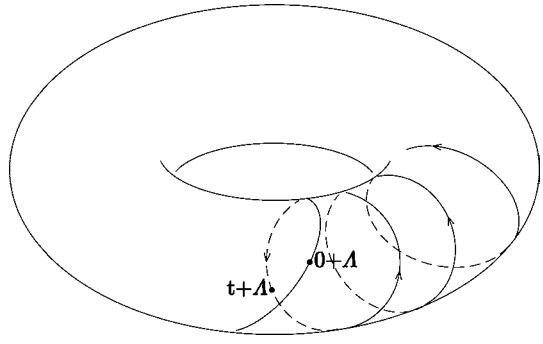

Figure 2
A fragment of the orbit of Λ as seen in the torus parameterization.

[2] Model sets can be taken more generally with any locally compact Abelian group as the internal space.

When we say that β is 1–1 almost everywhere, we mean that the set A of points ξ in $\mathbb{T}$, for which there is more than one point set over ξ, satisfies $\theta_{\mathbb{T}}(A) = 0$.

There is a *unique* $\mathbb{R}^d$-invariant ergodic measure μ on $X(\Lambda)$ with $\mu\big(X(\Lambda)\big) = 1$. In fact β relates μ and θ:

$$\beta(\mu) = \theta, \tag{13}$$

or more specifically, $\theta(A) = \mu(\beta^{-1}A)$ for all measurable subsets A of $\mathbb{T}$. With μ in hand, we can introduce the space $L^2\big(X(\Lambda), \mu\big)$ of square-integrable functions on $X(\Lambda)$. As already pointed out, the natural action of $\mathbb{R}^d$ on this is unitary.

3.2. From hulls to tori

Square-integrable functions on $X(\Lambda)$ and square-integrable functions on $\mathbb{T}$ can be identified:

$$L^2\big(X(\Lambda), \mu\big) \simeq L^2(\mathbb{T}, \theta). \tag{14}$$

The isomorphism is easy to understand:

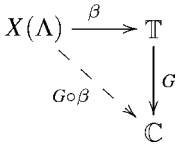

gives us a map

$$L^2(\mathbb{T}, \theta) \longrightarrow L^2\big(X(\Lambda), \mu\big).$$

Since β is almost everywhere 1–1, the map is a bijection.

This allows us to analyze functions on $X(\Lambda)$ by treating them as functions on $\mathbb{T}$. The advantage of this is that functions in $L^2(\mathbb{T}, \theta)$ have Fourier expansions

$$\widetilde{F}(z) = \sum_{\widetilde{k} \in \widetilde{L}^\circ} a_k \exp(2\pi i \langle \widetilde{k} \mid z \rangle), \quad z \in \mathbb{T},\ a_k \in \mathbb{C}. \tag{15}$$

Here $\langle \cdot \mid \cdot \rangle$ is the natural dot product on $\mathbb{R}^d \times \mathbb{R}^d = \mathbb{R}^{2d}$ and $\widetilde{L}^\circ$ is the lattice that is $\mathbb{Z}$-dual to $\widetilde{L}$:

$$\widetilde{k} \in \widetilde{L}^\circ \Longleftrightarrow \langle \widetilde{k} \mid \widetilde{x} \rangle \in \mathbb{Z} \quad \text{for all } \widetilde{x} \in \widetilde{L}.$$

Assuming that the dot product is rational valued on $\widetilde{L}$, this new lattice is in the $\mathbb{Q}$ span of $\widetilde{L}$ and its elements $\widetilde{k}$ have the same type of decompositions $\widetilde{k} = (k, k')$ as elements of $\widetilde{L}$. In particular, for each $\widetilde{k}$ there is a unique $k \in \mathbb{R}^d$. We prepare for the ultimate reduction of everything to the physical space by using the symbols a_k rather than $a_{\widetilde{k}}$ for the coefficients of the Fourier expansion. We shall write L° for the projection of $\widetilde{L}^\circ$ on the physical side, so we can just as well write $k \in L^\circ$ as $\widetilde{k} \in \widetilde{L}^\circ$. We will call L° the dual of L. The mapping $(\cdot)' : L^\circ \to \mathbb{R}^d$ here is compatible with that on L; indeed $\mathbb{Q}L^\circ = \mathbb{Q}L$.

The corresponding functions on $X(\Lambda)$ have similar expansions. This works as follows: If $F : X(\Lambda) \longrightarrow \mathbb{C}$ corresponds to $\widetilde{F} : \mathbb{T} \longrightarrow \mathbb{C}$ then, for $\Lambda_1 \in X(\Lambda)$ with $\beta(\Lambda_1) = (x, y)_L$, we have as L^2 functions

$$F(\Lambda_1) = \widetilde{F}\big((x, y)_L\big) = \sum_{k \in L^\circ} a_k \exp\big(2\pi i \langle \widetilde{k} \mid (x, y) \rangle\big). \tag{16}$$

3.3. Local functions on model sets

Let Λ be a model set arising from the cut-and-project scheme of equation (5). Let $\mathbb{T} = \mathbb{T}^{2d} = (\mathbb{R}^d \times \mathbb{R}^d)/L$ be the torus with torus parameterization

$$\beta : X(\Lambda) \longrightarrow \mathbb{T}.$$

Then we have the identification [equation (14)] of the corresponding L^2 spaces. Each element $\Lambda' \in X(\Lambda)$ maps by β to a point $\beta(\Lambda')$ in $\mathbb{T}$. We also know $\beta(\Lambda) = (0, 0)_L$ and $\beta(t + \Lambda) \to (t, 0)_L$, so we know how β works on $\mathbb{R}^d + \Lambda$.

Suppose f is a local function with respect to the model set Λ. From the local function f we have its extension $F \in L^2\big(X(\Lambda), \mu\big)$, which is continuous. Then we obtain $\widetilde{F} \in L^2(\mathbb{T}, \theta)$, where

$$\widetilde{F}\big((t, 0)_L\big) = \widetilde{F}\big(\beta(t + \Lambda)\big) = F(t + \Lambda) = f(t), \tag{17}$$

and we can write

$$\widetilde{F}(\cdot) = \sum_{k \in L^\circ} a_k \exp(2\pi i \langle \widetilde{k} \mid \cdot \rangle),$$

where L° is the dual of L.

Definition 3. The Fourier–Bohr expansion of the local function f is

$$\begin{aligned} f(t) = F(t + \Lambda) = \widetilde{F}\big((t, 0)_L\big) &= \sum_{k \in L^\circ} a_k \exp\big(2\pi i \langle \widetilde{k} \mid (t, 0) \rangle\big) \\ &= \sum_{k \in L^\circ} a_k \exp(2\pi i \langle k \mid t \rangle). \end{aligned} \tag{18}$$

Our study of almost periodic functions on Λ becomes the study of functions on $\mathbb{T}$ and their restrictions to the 'spiral' orbit $\mathbb{R}^d + \Lambda$ in $\mathbb{T}$ given by the embedding [equation (10)], *i.e.* restriction to $(\mathbb{R}^d, 0)_L$, see Fig. 2.

3.4. Fourier coefficients

Let us continue with the situation in §3.3. For all $x \in \mathbb{T}$,

$$\widetilde{F}(x) = \sum_{k \in L^\circ} a_k \exp(2\pi i \langle \widetilde{k} \mid x \rangle), \tag{19}$$

where

$$a_k = \int_{\mathbb{T}} \exp(-2\pi i \langle \widetilde{k} \mid x \rangle) \widetilde{F}(x)\, \mathrm{d}\theta_{\mathbb{T}}(x). \tag{20}$$

Unfortunately, we do not have total control over $\widetilde{F}$. We know it only on $(\mathbb{R}^d, 0)_L$. To compute a_k from f alone, we use the Birkhoff ergodic theorem:[3] for all continuous functions $\widetilde{G}$ on $\mathbb{T}$,

[3] It is hard to find convenient references for the Birkhoff ergodic theorem in the form we need it. Most references prove it over $\mathbb{Z}$ or $\mathbb{R}$. Keller (1998) gives a proof over $\mathbb{Z}^d$, which is easy to adapt to $\mathbb{R}^d$.

$$\int_{\mathbb{T}} \widetilde{G}(x)\,\mathrm{d}\theta_{\mathbb{T}}(x) = \lim_{R\to\infty} \frac{1}{\mathrm{vol}\,B_R} \int_{B_R} \widetilde{G}\big((t,0)_L\big)\,\mathrm{d}t. \qquad (21)$$

Thus

$$a_k = \lim_{R\to\infty} \frac{1}{\mathrm{vol}\,B_R} \int_{B_R} \exp\big(-2\pi i\langle \widetilde{k} \mid (t,0)\rangle\big)\,\widetilde{F}\big((t,0)_L\big)\,\mathrm{d}t$$
$$= \lim_{R\to\infty} \frac{1}{\mathrm{vol}\,B_R} \int_{B_R} \exp(-2\pi i\langle k \mid t\rangle)\,f(t)\,\mathrm{d}t. \qquad (22)$$

Here we use $F\big((t,0)_L\big) = f(t)$ and $\widetilde{k} = (k,k')$, so

$$\langle \widetilde{k} \mid (t,0)\rangle = \langle k,t\rangle + \langle k',0\rangle = \langle k,t\rangle.$$

The averaging sequence $\{B_R\}$ that we have employed here can be replaced by any unbounded ascending sequence $\{A_n\}$, where $A_n \subset \mathbb{R}^d$ is compact, $\bigcup A_n = \mathbb{R}^d$, and the boundary of A_n has measure 0 for all n. In practice one should adapt the averaging sequence to the problem at hand.

4. Discretization

4.1. Main components

Our objective is to devise a discrete method by which to estimate the coefficients a_k of equation (22) of a local function f with respect to a model set $\Lambda = \Lambda(\Omega)$. This means replacing the integral by a finite sum of values of the integrand. The problem is to do this in such a way that it respects the cut-and-project scheme in which the model set lives, can be guaranteed to converge in the limit to the required integral, and can be carried out efficiently from a computational point of view.

There are three components to this:

(i) deciding on a suitable domain of integration (what should we use for B_R?);

(ii) creating the points of evaluation of the integrand, including how many there should be;

(iii) deciding to which set of Fourier coefficients (which values of k) we should restrict our attention.

A key feature of discrete methods involving periodic functions is the use of finite groups arising from refinements of the period lattice and quotients of its dual lattice (*e.g.* Moody & Patera, 2006). We need to translate this concept into the context of cut-and-project schemes. The set of points on which the integrand is evaluated is created out of the same cut-and-project process that creates the original model set. The ingredients are a choice of a suitable lattice $\widetilde{L}_N \supset \widetilde{L}$, which then gives rise to the finite group $\widetilde{L}_N/\widetilde{L}$. The data points in $\mathbb{R}^d$ at which computations of our functions will be made come by projection into physical space of a suitable set of coset representatives of $\widetilde{L}_N$ modulo $\widetilde{L}$. The corresponding frequencies (wavevectors) k are chosen from the dual lattice L°. The choice of values of k at which we should evaluate the Fourier coefficients a_k come by selecting suitable representatives of $\widetilde{L}^\circ$ modulo $\widetilde{L}^\circ_N$. The key point is the duality

$$\langle \cdot \mid \cdot \rangle : \widetilde{L}^\circ/\widetilde{L}^\circ_N \times \widetilde{L}_N/\widetilde{L} \longrightarrow (1/N)\mathbb{Z}/\mathbb{Z}.$$

4.2. Outline of the discretization process

In this section we give more precise details as to how the goals of §4.1 can be achieved. The process necessarily involves a number of decisions, which can only be made in the context of the situation at hand. In §§5 and 6 we shall see how this looks in particular examples.

It should be noted that, although setting up the computational details is somewhat involved, these details depend only on the cut-and-project scheme and the degree of accuracy required from the computation. Once this is established the data points and choices of frequencies are already determined, and they suffice for the Fourier analysis of *all* functions that arise out of the same almost periodic family and are algorithmically easy to compute.

We begin with the cut-and-project scheme [equation (5)] with torus $\mathbb{T}$ and note the natural extension of the mapping $(\cdot)'$ to the rational span of the module L:

$$\begin{array}{ccccc} \mathbb{Q}L & \overset{1-1}{\longleftarrow} & \mathbb{Q}\widetilde{L} & \longrightarrow & \mathbb{Q}\widetilde{L}' \\ x & \longmapsto & \tilde{x} = (x,x') & \longmapsto & x'. \end{array} \qquad (23)$$

We assume that $\mathbb{R}^{2d} \simeq \mathbb{R}^d \times \mathbb{R}^d$ is supplied with the standard dot product (denoted $\langle \cdot \mid \cdot \rangle$), and then define the dual lattice:

$$\widetilde{L}^\circ = \{Y \in \mathbb{R}^d \times \mathbb{R}^d : \langle Y \mid \widetilde{x}\rangle \in \mathbb{Z} \quad \text{for all } \widetilde{x} \in \widetilde{L}\}.$$

Then $\widetilde{L}^\circ$ is a $\mathbb{Z}$-module of the same rank as $\widetilde{L}$, namely $2d$. There is a cut-and-project scheme dual to equation (5) of which $\widetilde{L}^\circ$ is the lattice (Moody, 1997):

$$\begin{array}{ccccc} \mathbb{R}^d & \overset{\|}{\longleftarrow} & \mathbb{R}^d \times \mathbb{R}^d & \overset{\perp}{\longrightarrow} & \mathbb{R}^d \\ & & \cup & & \\ L^\circ & \overset{1-1}{\longleftarrow} & \widetilde{L}^\circ & \overset{\text{dense image}}{\longrightarrow} & (L^\circ)'. \end{array} \qquad (24)$$

We shall use the same type of notation as in equation (23) for this scheme too. It arises by taking the Pontryagin duals of all the groups in equation (23), whereupon $\widetilde{L}^\circ$ appears as the dual of the torus $\mathbb{T}$. For more on dual cut-and-project schemes see Moody (1997).

Dualizing can be considerably simplified if the inner product on $\mathbb{R}^d \times \mathbb{R}^d$ is rational valued on the lattice $\widetilde{L}$. This quite often happens in practice. For instance, it occurs in the Fibonacci example below, where the inner product arises from the trace form on $\mathbb{Q}[\sqrt{5}]$. When this arises one can identify $\widetilde{L}^\circ$ as a subset of $\mathbb{Q}\widetilde{L}$ and thereby avoid having to find the new $(\cdot)'$ mapping. However, in the general situation such simplifications need not exist, and we do not assume them here.

In reading what follows it is good to keep in mind the equation

$$\exp(2\pi i\langle \widetilde{k} \mid \widetilde{s}\rangle) = \exp(2\pi i\langle k \mid s\rangle)\exp(2\pi i\langle k' \mid s'\rangle), \qquad (25)$$

which lies at the bottom of the approximation. The discrete Fourier analysis is accomplished by a dual pair of finite groups from which $\widetilde{k}$ and $\widetilde{s}$ will come. The actual values of $\widetilde{k}$ and $\widetilde{s}$ are important only modulo the lattices $\widetilde{L}^\circ_N$ and $\widetilde{L}$, respectively, and this freedom lies at the heart of the process.

The values of s should be in the range A of our integration, and ideally we would have the corresponding $s' = 0$ since the $\widetilde{s}$

are supposed to be representing points of the physical space $\mathbb{R}^d$. However, the latter is not possible, so we attempt to choose the $s \in A$ along with s' as small as possible. The approximation then works by throwing away the term that involves k', s' in equation (25). The set of values of $\widetilde{k}$ is constrained primarily by the requirement that the values of $|k|$ should be small; see the discussion after Step 5 below.

4.3. The six steps

Step 1. Choose a finite subgroup of $\mathbb{T}$ of order N. This appears in the form $\widetilde{L}_N/\widetilde{L}$ where $\widetilde{L}_N \supset \widetilde{L}$ is a lattice refining $\widetilde{L}$. The number N will determine the number of points of evaluation in approximating the integrals by sums. We have $\widetilde{L}_N \subset \mathbb{Q}\widetilde{L}$, and it has a $\mathbb{Z}$-dual $\widetilde{L}_N^\circ \subset \widetilde{L}^\circ$ which is of index N in $\widetilde{L}^\circ$.

This affords the natural pairing

$$\widetilde{L}^\circ/\widetilde{L}_N^\circ \times \widetilde{L}_N/\widetilde{L} \longrightarrow (1/N)\mathbb{Z}/\mathbb{Z} \tag{26}$$

induced by $\langle \cdot \mid \cdot \rangle$ (and still denoted by $\langle \cdot \mid \cdot \rangle$). Using the $(\cdot)'$ mappings, we obtain, in the obvious notation, the $\mathbb{Z}$-modules $L_N \supset L$, $L_N^\circ \subset L^\circ$, $\widetilde{L}_N/\widetilde{L} \simeq L_N/L$, $\widetilde{L}^\circ/\widetilde{L}_N^\circ \simeq \widetilde{L}/\widetilde{L}_N$, and an induced pairing

$$\langle \cdot \mid \cdot \rangle : L^\circ/L_N^\circ \times L_N/L \longrightarrow (1/N)\mathbb{Z}/\mathbb{Z}.$$

Replacing $\widetilde{L}$ by $\widetilde{L}_N$, we have the refined cut-and-project scheme

$$\begin{array}{ccccc} \mathbb{R}^d & \longleftarrow & \mathbb{R}^d \times \mathbb{R}^d & \longrightarrow & \mathbb{R}^d \\ & & \cup & & \\ L_N & \overset{1-1}{\longleftrightarrow} & \widetilde{L}_N & \longleftrightarrow & L'_N \end{array} \tag{27}$$

and similarly its dual.

Step 2. Choose a fundamental domain C for $\widetilde{L}$. A canonical choice would be the Voronoi cell of $\widetilde{L}$ at 0, but any other choice is allowable. In the examples below we use the parallelogram defined by a pair of basis vectors of $\widetilde{L}$. Cover $(\mathbb{R}^d, 0) \subset \mathbb{R}^{2d}$ with a set of translates $\widetilde{t} + C$ of C by elements of $\widetilde{L}$. The projection of these cells into the physical space $\mathbb{R}^d$ covers it, though in general the projected $\widetilde{t} + C$ have many overlaps.

Step 3. Form $\widetilde{S} := \widetilde{L}_N \cap C$. This provides a complete set of representatives in $\widetilde{L}_N$ for the group $\widetilde{L}_N/\widetilde{L}$.

Step 4. Choose a region A which will delimit the range over which the Fourier coefficients of f will be estimated in the form

$$a_k = a_{\tilde{k}} \simeq \frac{1}{\operatorname{vol} A} \int_A \exp(-2\pi i \langle k \mid t \rangle) f(t)\, \mathrm{d}t.$$

These integrals have to be computed for values of k that come from L°/L_N°.

Take as A the image of a finite set of the translates of C appearing in Step 2, *i.e.*

$$A = \Big(\bigcup_{\tilde{t} \in \tilde{T}} \widetilde{t} + C \Big)^{\shortparallel}$$

for some finite subset of $\widetilde{T}$ elements of $\widetilde{L}$. The choice of A is again determined by the problem at hand.

We need next to determine a set of data points in $\mathbb{R}^d$ which will serve to replace the integrals of Step 4 by finite sums. This is the purpose of the next step.

As we pointed out above, we are free to translate the elements of $\widetilde{S}$ by $\widetilde{L}$ as we please, and we wish to do this so that the projected images are in our region of integration, $A = \bigcup_{\tilde{t} \in \tilde{T}} (\widetilde{t} + C)^{\shortparallel}$. We also keep in mind that we wish to do this so as to minimize the size of the corresponding s'.

Step 5. For each $\widetilde{s} = (s, s') \in \widetilde{S}$ find a $\widetilde{t(s)} \in \widetilde{T}$ for which $|s' + t(s)'|$ is minimal. Then the set of data points is

$$D := \{ s + t(s) : \widetilde{s} \in \widetilde{S} \}.$$

At this point, for each $k \in L^\circ$ we have

$$a_k := \frac{1}{\operatorname{vol} A} \sum_{u \in D} \exp(-2\pi i \langle k \mid u \rangle) f(u)$$

and the resulting approximation of f is

$$f(x) \simeq \sum_{k \in K} a_k \exp(2\pi i \langle k \mid x \rangle).$$

The set K is to run over a complete set of representatives of L°/L_N°. The choice seems free, but one may assume that in most cases the lower frequencies (smaller $|k|$) are most essential in approximating f by using only finitely many of its frequencies. For this reason we have:

Step 6. Choose k for each class of L°/L_N° with $|k|$ taken as small as possible.

This concludes the broad description of the algorithm.

5. A Fibonacci example

To make all this more concrete we work through the details of a one-dimensional example, the well known Fibonacci sequence, where the cut-and-project scheme lives in two dimensions and the geometry of the data set D and the set of translates $\widetilde{T}$ *via* a refinement lattice and new windows are easily visualized. This involves first setting up the cut-and-project scheme in detail (§5.1 and §5.2) and then describing a Fibonacci point set arising from the standard Fibonacci substitution in terms of it (§5.3). We then follow steps 1 through 6 of §4.3, which provide the data points and corresponding frequencies that will work for the analysis of any local function that we may choose. In §6 we apply this information to two simple examples of local functions to see how well the methods actually work.

One of the great virtues of the cut-and-project method is that it is primarily an algebraic tool and does not require great geometric insight to use it. Given that for aperiodic structures in dimension greater than one we are almost always in the situation of lattices of rank greater than three, and hence are forced into spaces in dimensions greater than three, this type of algebraic formalism is of enormous value. However, in the Fibonacci example, in which everything can be performed in two dimensions, it is useful to see the underlying geometry explicitly. Thus we have gone to some effort to show the geometric meaning of the central feature of the method, that is, the creation of the data points, and to show what the

approximations look like and how good they are in comparison with exact computation. In practice all this is unnecessary. The only part of the algorithm that requires any serious insight into the geometry (and it is actually trivial in the Fibonacci example) is the selection of the fundamental domain and the translates of it that are to be used. It is their projection that makes the domain in physical space in which the data will lie.

5.1. The Fibonacci cut-and-project scheme

Let $\tau := \frac{1}{2}(1+\sqrt{5})$ and let $Z[\tau] = \mathbb{Z} + \mathbb{Z}\tau$. Then $Z[\tau]$ is the ring of integers of the field $\mathbb{Q}[\tau] = \mathbb{Q}[\sqrt{5}]$ and $\tau^2 = \tau + 1$. Let $(\cdot)'$ on $Z[\tau]$ and $\mathbb{Q}[\tau]$ be the conjugation that interchanges $\sqrt{5}$ and $-\sqrt{5}$.

We define

$$\widetilde{\mathbb{Z}[\tau]} := \{(x, x') : x \in \mathbb{Z}[\tau]\} \subset \mathbb{R} \times \mathbb{R}.$$

$\widetilde{\mathbb{Z}[\tau]}$ is a lattice in $\mathbb{R} \times \mathbb{R}$ and its natural projections

$$\mathbb{R} \longleftarrow \mathbb{R} \times \mathbb{R} \longmapsto \mathbb{R}$$

into $\mathbb{R}$ provide the setup for the Fibonacci cut-and-project scheme:

$$\begin{array}{ccccc} \mathbb{R} & \longleftarrow & \mathbb{R} \times \mathbb{R} & \longrightarrow & \mathbb{R} \\ \cup & & \cup & & \cup \\ \mathbb{Z}[\tau] & \longleftarrow & \widetilde{\mathbb{Z}[\tau]} & \longrightarrow & \mathbb{Z}[\tau] \\ x & \longleftarrow & \tilde{x} = (x, x') & \longmapsto & x' \end{array} \tag{28}$$

A natural basis of $\widetilde{\mathbb{Z}[\tau]}$ is $\{(1,1), (\tau, \tau')\}$ and the standard inner product on $\widetilde{\mathbb{Z}[\tau]}$ is defined by

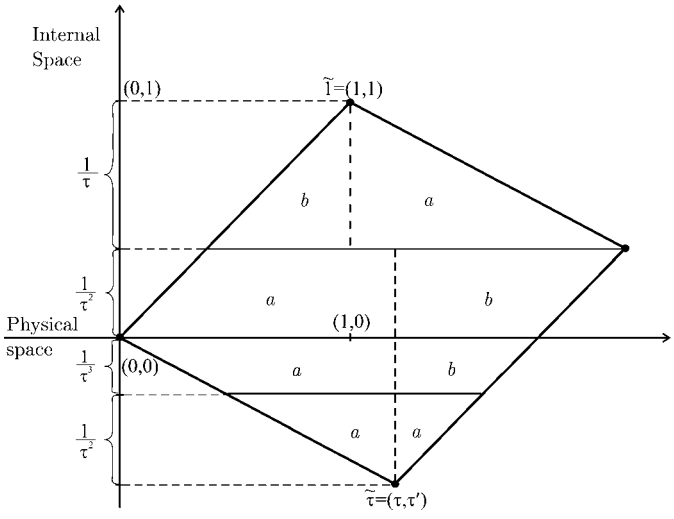

Figure 3
The fundamental cell C of the lattice $\widetilde{\mathbb{Z}[\tau]} = \mathbb{Z}(1,1) + \mathbb{Z}(\tau, \tau')$ is shown in terms of the standard coordinate system for $\mathbb{R} \times \mathbb{R}$. When C is imagined as a torus by identifying opposite sides and the physical space is wrapped onto it using these identifications, then the a and b regions shown here indicate which parts of the physical space are lying in a or b tiles, respectively.

$$(\tilde{x} \mid \tilde{y}) = (2x \cdot y)_{\mathbb{Z}} = \delta xy + (\delta xy)'. \tag{29}$$

Here the notation $(\cdot)_{\mathbb{Z}}$ indicates taking the rational component a of $2x \cdot y \in \mathbb{Z}[\tau] =: a + b\tau$, and

$$\begin{aligned} \delta &= (\tau\sqrt{5})^{-1} = \big(\tau(\tau - \tau')\big)^{-1} = (\tau^2 + 1)^{-1}, \\ \delta' &= (-\tau'\sqrt{5})^{-1} = \big(\tau'(\tau' - \tau)\big)^{-1} = (\tau'^2 + 1)^{-1}. \end{aligned} \tag{30}$$

In particular,

$$(\tilde{1} \mid \tilde{1}) = \big(2(1 \cdot 1)\big)_{\mathbb{Z}} = 2, \quad (\tilde{\tau} \mid \tilde{\tau}) = (2\tau^2)_{\mathbb{Z}} = 2,$$
$$(\tilde{1} \mid \tilde{\tau}) = (2\tau)_{\mathbb{Z}} = 0.$$

The geometry of the fundamental cell for the lattice $\widetilde{\mathbb{Z}[\tau]}$ is illustrated in Fig. 3. Chen *et al.* (1998) give further details of the material discussed here.

5.2. The dual lattice

The inner product $(\cdot \mid \cdot)$ allows us to identify $\widetilde{\mathbb{Z}[\tau]}^\circ$ inside the rational span of $\widetilde{\mathbb{Z}[\tau]}$ and to express $\langle \cdot \mid \cdot \rangle$ in terms of $(\cdot \mid \cdot)$. The basis dual to $\{(1,1), (\tau, \tau')\}$ is given by

$$\tilde{\omega}_1 = \frac{1}{2}\tilde{1} = \left(\frac{1}{2}, \frac{1}{2}\right), \qquad \tilde{\omega}_2 = \frac{1}{2}\tilde{\tau} = \left(\frac{\tau}{2}, \frac{\tau'}{2}\right), \tag{31}$$

and the dual lattice is

$$(\widetilde{\mathbb{Z}[\tau]})^\circ = \mathbb{Z}\tilde{\omega}_1 + \mathbb{Z}\tilde{\omega}_2 = \tfrac{1}{2}\widetilde{\mathbb{Z}[\tau]}. \tag{32}$$

The elements of $(\widetilde{\mathbb{Z}[\tau]})^\circ$ are always of the form $\tilde{k} = (k, k')$, and we can write

$$\mathbb{Z}[\tau]^\circ := \{k : \tilde{k} = (k, k') \in (\widetilde{\mathbb{Z}[\tau]})^\circ\}. \tag{33}$$

Then

$$(\widetilde{\mathbb{Z}[\tau]})^\circ = \widetilde{\mathbb{Z}[\tau]^\circ} = \{\tilde{k} : k = (k, k') \in \mathbb{Z}[\tau]^\circ\},$$

and $\langle \tilde{k} \mid \tilde{x} \rangle$ becomes $(\tilde{k} \mid \tilde{x})$, which is more useful notation for the following.

The 2-torus $\mathbb{T}$ of the cut-and-project scheme [equation (28)] is then

$$\mathbb{T} = (\mathbb{R} \times \mathbb{R})/\widetilde{\mathbb{Z}[\tau]}.$$

Fourier series on $\mathbb{T}$ are expressed in terms of the characters $\chi_{\tilde{k}}$, namely

$$\chi_{\tilde{k}}(\tilde{x}) = \exp\big(2\pi i(\tilde{k} \mid \tilde{x})\big), \quad \text{where } \tilde{k} = (k, k') \in \mathbb{Z}\tilde{\omega}_1 + \mathbb{Z}\tilde{\omega}_2. \tag{34}$$

Here $\tilde{x}$ can be arbitrary in $\mathbb{R} \times \mathbb{R}$, but we shall need to compute only with $\tilde{x} \in \mathbb{Q}\tilde{\omega}_1 + \mathbb{Q}\tilde{\omega}_2$ for which $\tilde{}$ is well defined [equation (28)]. For these elements $(\tilde{k} \mid \tilde{x}) = (2k \cdot x)_{\mathbb{Q}}$.

The product $(\cdot \mid \cdot)$ extends to $\mathbb{R} \times \mathbb{R}$, but care has to be taken. For a typical element $a\tilde{1} + b\tilde{\tau}$, $a, b \in \mathbb{R}$ of our superspace $\mathbb{R} \times \mathbb{R}$ the inner product is calculated as

$$\big((a\tilde{1} + b\tilde{\tau}) \mid (c\tilde{1} + d\tilde{\tau})\big) = 2ac + 2bd,$$

where

$$a\tilde{1} + b\tilde{\tau} = a(1,1) + b(\tau, \tau') = (a + b\tau, a + b\tau') \in \mathbb{R} \times \mathbb{R}.$$

Consider

$$\widetilde{k} = a\widetilde{\omega}_1 + b\widetilde{\omega}_2 = \frac{a}{2}\widetilde{1} + \frac{b}{2}\widetilde{\tau} = \left(\frac{a+b\tau}{2}, \frac{a+b\tau'}{2}\right) = (k, k') \in \widetilde{\mathbb{Z}[\tau]}^\circ,$$

where $a, b \in \mathbb{Z}$. Suppose we want to compute $(\widetilde{k} \mid (t, 0)), t \in \mathbb{R}$. From

$$(1, 0) = \frac{1}{\tau\sqrt{5}}\widetilde{1} + \frac{1}{\sqrt{5}}\widetilde{\tau} = \delta\widetilde{1} + \tau\delta\widetilde{\tau},$$
$$(0, 1) = \tau^2\delta\widetilde{1} - \tau\delta\widetilde{\tau} = \delta'\widetilde{1} + \tau'\delta'\widetilde{\tau},$$

where δ, δ' are from equation (30), we have

$$\big(\widetilde{k} \mid (1, 0)\big) = 2\delta k,$$

and so

$$\big(\widetilde{k} \mid (t, 0)\big) = 2\delta k t \quad \text{for all } t \in \mathbb{R}.$$

We are interested in model sets Λ coming from the cut-and-project scheme [equation (28)]. In the context of equation (28), the Fourier–Bohr expansion [equation (18)] assumes the simpler form

$$f(t) = F(t + \Lambda) = \widetilde{F}\big((t, 0)_{\widetilde{\mathbb{Z}[\tau]}}\big) = \sum_{k \in \mathbb{Z}[\tau]^\circ} a_k \exp(2\pi i 2\delta k t). \quad (35)$$

We shall use a_k computed in the form

$$a_k = \lim_{R\to\infty} (1/R) \int_0^R \exp(-2\pi i 2kt) f(t)\, \mathrm{d}t.$$

For future use note that

$$\big(\widetilde{k} \mid (0, 1)\big) = \left(\left(\frac{a+b\tau}{2}, \frac{a+b\tau'}{2}\right) \middle| \delta'\widetilde{1} + \tau'\delta'\widetilde{\tau}\right) = 2k'\delta',$$
$$\big(\widetilde{k} \mid (0, u)\big) = 2uk'\delta'. \quad (36)$$

5.3. The Fibonacci model set

The standard two-letter Fibonacci sequence is the fixed point of the substitution $a \to ab$, $b \to a$: namely,

$$abaababa \ldots.$$

With tile lengths τ for a symbols and 1 for b symbols, and starting at 0, we obtain the sequence of tiles that cover the non-negative part of the real line. The left-hand ends of these tiles,

$$0,\ \tau,\ \tau{+}1,\ 2\tau{+}1,\ 3\tau{+}1,\ 3\tau{+}2,\ 4\tau{+}2,\ 4\tau{+}3,\ 5\tau{+}3,\ \ldots$$

form an infinite sequence of points on the non-negative real line. This set appears explicitly as the non-negative part of the model set

$$\Lambda = \Lambda([-1, 1/\tau))$$

arising from the cut-and-project scheme [equation (28)].[4] Λ decomposes as $\Lambda_a = \Lambda([-1/\tau^2, 1/\tau))$ and $\Lambda_b = \Lambda([-1, -1/\tau^2))$, which give the left-hand end points of the a and b tiles, respectively.

A useful and commonly used way to visualize the distribution of a and b points is to view them on the torus $\mathbb{T}$ after embedding [equation (10)] of $\mathbb{R}$ in $\mathbb{T}$. The fundamental cell (see Fig. 3) with opposite edges identified is $\mathbb{T}$. To see Λ itself being formed, we start at $(0, 0)$ and trace out $(t, 0)$, $t \in \mathbb{R}$, with the usual rules for exiting and re-entering the fundamental cell. We move continuously. Our moving point has three 'whiskers' attached to it.

$a(1)$: a whisker of length $1/\tau$ facing vertically upwards;

$a(2)$: a whisker of length $1/\tau^2$ facing down;

$b(1)$: a whisker of length $1/\tau$ that faces down, but has an initial gap of size $1/\tau^2$.

The rule is this. As our point moves along the line on the fundamental cell, if the $a(1)$ whisker hits $(1, 1)$ [*i.e.* $(1, 1)$ is close enough to get cut by this whisker], we get an a point of Λ. If the $a(2)$ whisker hits the point (τ, τ'), we also get an a point of Λ. If the $b(1)$ whisker hits the point (τ, τ'), we get a b point.

Essentially the window, represented by the whiskers, is carried along with the moving point, and exits and re-enters the fundamental cell with the moving point.

The advantage of this point of view is that it allows us to divide the fundamental cell into regions that deliver the a and b points, and thus to see what our function $f(t)$ looks like on the fundamental cell.

In Fig. 3 the vertical dotted lines are the key thing. Our moving point moves to the right, and every time it crosses a dotted vertical line we get a new point of Λ, thus starting a new interval. We stay on that interval until the next crossing.

The a and b regions are indicated in Fig. 3.

5.4. Discretization

We now go in to the details of how to deal with the Fourier analysis using discrete methods. Here we follow the six steps outlined in §4.3.

Write $\widetilde{L}$ for $\widetilde{\mathbb{Z}[\tau]}$, so $\widetilde{L} = \mathbb{Z}\widetilde{1} + \mathbb{Z}\widetilde{\tau}$. Let

$$C := \{u\widetilde{1} + v\widetilde{\tau} : 0 \le u, v < 1\}$$

be a fundamental region for $\widetilde{L}$. Its volume is equal to $\sqrt{5}$.

Fix any $N \in \mathbb{Z}_+$. We want to create a lattice $\widetilde{L}_N$ that is a refinement of $\widetilde{L}$. In §4.3 we took $\widetilde{L}_N \supset \widetilde{L}$ with $[\widetilde{L}_N : \widetilde{L}] = N$. In our present situation we use the most obvious lattices, namely $(1/N)L$. These actually have index N^2, so there are some slight notational differences between this section and §4.3. Since $N\widetilde{L}_N \subseteq \widetilde{L}$, so $\widetilde{L}_N \subset \mathbb{Q}\widetilde{1} + \mathbb{Q}\widetilde{\tau}$.

Let $\widetilde{S} := L_N \cap C$, so $\widetilde{S}$ is a complete set of representatives of $L_N \bmod L$.

Together this completes Steps 1, 2 and 3 of §4.2.

To aid a better understanding of the approximations we also introduce a fundamental region C_N for L_N, chosen so that

$$C = \bigcup_{\tilde{s} \in \tilde{S}} \tilde{s} + C_N. \quad (37)$$

[4] Alternatively one can use $\Lambda((-1, 1/\tau])$, which differs from Λ in the two points coming from the ends of the interval $[-1, 1/\tau)$. This is an example of a pair of sets that map to the same place in $\mathbb{T}$. This ambiguity shows up in an interesting way later on (see §6.3).

For Step 4 we choose as our delimiting range in $\mathbb{R}$ an interval $[0, R]$, where R is a positive real number taken so that $(R, 0)$ taken modulo $\widetilde{L}$ is on the boundary of C. Following along the path $(t, 0)$, $t \in \mathbb{R}_{>0}$, and wrapping around C as indicated in Fig. 4, this amounts to stopping at some point R where the path is just exiting C, so that we have an exact number of passes of C. Thus the path $(t, 0)$, $0 \le t \le R$, involves an explicit set of translates $\widetilde{t}_i + C$, $i = 1, \ldots, M$ of C. Let $\widetilde{T} = \{\widetilde{t}_1, \ldots, \widetilde{t}_M\}$.

Let $f : \mathbb{R} \to \mathbb{C}$ be any continuous local function with respect to the model set $\Lambda = \Lambda([-1, 1/\tau))$, and let $\widetilde{F} : \mathbb{T} \to \mathbb{C}$ be its extension to a continuous function on $\mathbb{T} = \mathbb{R}^2/\widetilde{L}$. Generally we are interested in Fourier decomposition of $\widetilde{F}$ and along with it the corresponding decomposition of f. Thus we wish to compute expressions like

$$\int_{\mathbb{T}} \widetilde{F}(x) \exp\left(-2\pi i(\widetilde{k} \mid x)\right) \mathrm{d}\theta_{\mathbb{T}}(x).$$

Here $\widetilde{F}(\cdot) \exp\left(-2\pi i(\widetilde{k} \mid \cdot)\right)$ is just some other continuous function on $\mathbb{T}$ that is local with respect to Λ. Thus it suffices to deal with some general continuous function $\widetilde{G}$ on $\mathbb{T}$ and its restriction $g(t) = \widetilde{G}\big((t, 0)\big)$ to the line $(\mathbb{R}, 0) \bmod \widetilde{L}$.

Let

$$\varepsilon_N := \sup_{i=1,\ldots,N^2} \sup_{x \in \widetilde{s}_i + C_N} \left|\widetilde{G}(x) - \widetilde{G}(\widetilde{s}_i)\right|.$$

Our first estimate is

$$\int_{\mathbb{T}} \widetilde{G}\, \mathrm{d}\theta_{\mathbb{T}} \simeq (\sqrt{5}/N^2) \sum_{i=1}^{N^2} \widetilde{G}(\widetilde{s}_i).$$

Since $\operatorname{vol} C_N = \sqrt{5}/N^2$, the error in this is estimated by

$$\begin{aligned} &\left| \int_{\mathbb{T}} \widetilde{G}\, \mathrm{d}\theta - (\sqrt{5}/N^2) \sum_{i=1}^{N^2} \widetilde{G}(\widetilde{s}_i) \right| \\ &\quad = \left| \sum_{i=1}^{N^2} \int_{\widetilde{s}_i + C_{N^2}} \left(\widetilde{G}(x) - \widetilde{G}(\widetilde{s}_i)\right) \mathrm{d}\theta(x) \right| \\ &\quad \le \sum_{i=1}^{N^2} \int_{\widetilde{s}_i + C_{N^2}} \varepsilon_N\, \mathrm{d}\theta = \sum_{i=1}^{N^2} \varepsilon_N \operatorname{vol} C_{N^2} = \sqrt{5}\, \varepsilon_N, \end{aligned} \quad (38)$$

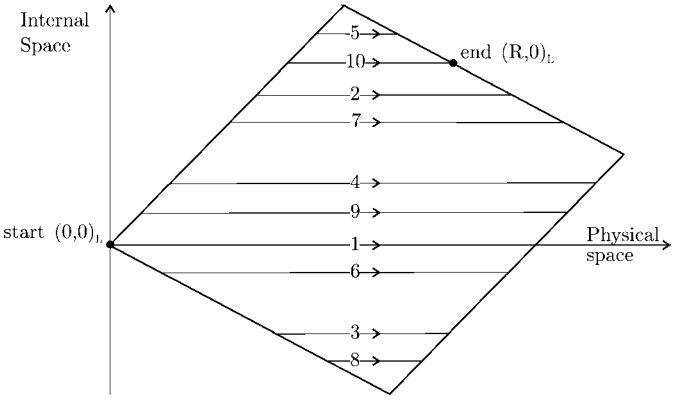

Figure 4
Ten crossings of C by the path $\{(t, 0)_L : 0 \le t \le R\}$ are shown in the torus. (Opposite sides of the parallelogram coincide.)

i.e. the error in our approximation is bounded by $\sqrt{5}\varepsilon_N$. In practice L_N and N would be chosen so as to provide a suitably *a priori* assigned value of ε_N.

5.5. Restriction to *f*

In order to be useful, the computation must be restricted to values of the function f, since this is all that one is given in practice. We wish to use an approximation of the form

$$(1/R) \int_0^R g(t)\, \mathrm{d}t = (1/R) \int_0^R \widetilde{G}(t, 0)\, \mathrm{d}t \simeq \int_{\mathbb{T}} \widetilde{G}\, \mathrm{d}\theta_{\mathbb{T}},$$

in accordance with equation (21).

In this section we indicate the geometry behind Step 5. Again, it should be pointed out that in the final analysis much of the detail that appears here need not appear at all in the actual algorithm.

The path $\{(t, 0)_L : 0 \le t \le R\}$, wrapped around C, is divided by C into segments $l_1, \ldots, l_M$.

Let $b_1 < b_2 < \ldots < b_M$ be the projections onto internal space of the boundary cutting points of $\{(t, 0) : 0 \le t \le R\}$ (Fig. 5). Define

$$c_0 = \tau', \;\; c_1 = \frac{b_1 + b_2}{2}, \ldots, \;\; c_{M-1} = \frac{b_{M-1} + b_M}{2}, \;\; c_M = 1.$$

The strips S_i formed by passing the interval $[c_{i-1}, c_i)$ in internal space through C in the direction of the physical axis form a partition of C. Through each strip in C runs a part l_i of our line $\{(t, 0)_L : 0 \le t \le R\}$. The idea is to use the intervals $[c_{i-1}, c_i)$ as windows and the line segments l_i as (part of) the physical space for a model set construction based on the lattice $\widetilde{L}_N$ (see Fig. 6). This will then produce the points on l_i that will be our data points for the evaluation of the functions $\widetilde{G}$ and then g. In other words, we are implicitly using the partial model sets $\Lambda_{\widetilde{L}_N}(S_i) \cap l_i$.

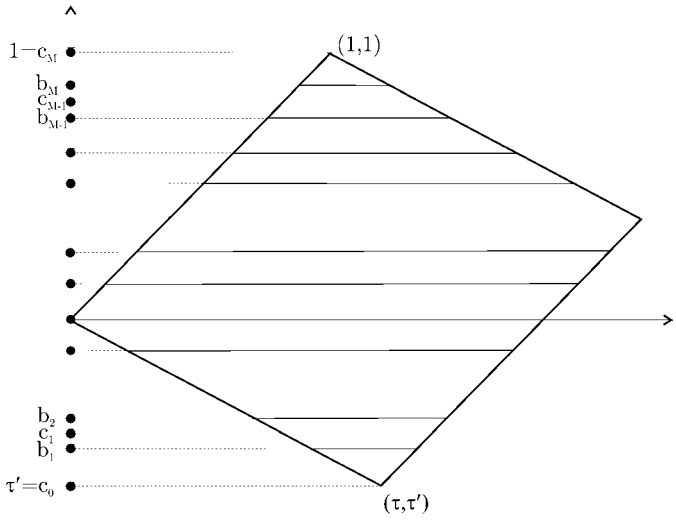

Figure 5
The projections $b_1, \ldots, b_M$ into internal space of the boundary cutting points of the path. The points $c_0, \ldots, c_M$ mark the boundaries of the smaller windows into which the original window $[\tau', 1)$ is partitioned.

Let $m(R) := \max\{|c_i - c_{i-1}|\}$ and

$$\varepsilon'_N := \sup_i \sup_{(x,v),(x,u)\in S_i} \left|\widetilde{G}(x,v) - \widetilde{G}(x,u)\right|, \quad i = 1, \ldots, M.$$

Each $\widetilde{s}_j \in \widetilde{S}$ lies in exactly one strip S_i. Let (p_j, q_j) be its projection onto the line segment l_i. Then $(p_j, q_j) \equiv (u_j, 0)_L$ for some $u_j \in [0, R]$. Thus we obtain $\{(u_1, 0), \ldots, (u_{N^2}, 0)\}$ on our path $\{(t, 0)_L : 0 \le t \le R\}$ (Fig. 6).

We have the estimate (38). Moreover,

$$\frac{\sqrt{5}}{N^2}\sum_{i=1}^{N^2} \widetilde{G}(\widetilde{s}_i) = \frac{\sqrt{5}}{N^2}\sum_{i=1}^{N^2} \big(\widetilde{G}(\widetilde{s}_i) - \widetilde{G}(p_i, q_i)\big) + \frac{\sqrt{5}}{N^2}\sum_{i=1}^{N^2} g(u_i),$$

since

$$\widetilde{G}(p_i, q_i) = \widetilde{G}\big((u_i, 0)\big) = g(u_i).$$

Thus

$$\left|\frac{\sqrt{5}}{N^2}\sum_{i=1}^{N^2} \widetilde{G}(\widetilde{s}_i) - \frac{\sqrt{5}}{N^2}\sum_{i=1}^{N^2} g(u_i)\right| \le \frac{\sqrt{5}}{N^2}\sum_{i=1}^{N^2} \varepsilon'_N = \sqrt{5}\,\varepsilon'_N, \quad (39)$$

since $\widetilde{s}_i$ and (p_i, q_i) both have a second component in the same interval $[c_{i-1}, c_i)$.

Combining equations (38) and (39), we have

$$\left|\int_{\mathbb{T}} \widetilde{G}\,\mathrm{d}\theta - \frac{\sqrt{5}}{N^2}\sum_{i=1}^{N^2} g(u_i)\right| < \sqrt{5}(\varepsilon_N + \varepsilon'_N). \quad (40)$$

This provides a method of estimating the integral $\int_{\mathbb{T}} \widetilde{G}\,\mathrm{d}\theta$ using only g on $[0, R]$ along with well chosen points in the interval. The two parameters N and R control the estimates.

In spite of the apparent complexity of strips, what is going on is easy to implement. For each $\widetilde{s}_i = (s_i, s'_i)$ there is a translation vector $\widetilde{t}_j \in \widetilde{T}$ for which $|s'_i + t'_j|$ is minimal. The corresponding data point is then $u_i := s_i + t_j$. This is Step 5 of §4.2.

6. Two explicit examples

6.1. Computation of Fourier coefficients

In this section we apply the methods outlined above to two almost periodic functions $f : \mathbb{R} \to \mathbb{R}$, both local with respect to the model set $\Lambda = \Lambda([-1, 1/\tau))$ of §5.3. The first is the distance-to-the-nearest-neighbor function

$$f(t) = \text{the distance of } t \text{ to the nearest point of } \Lambda. \quad (41)$$

This is a continuous and piecewise linear function that is local with respect to Λ.

The second is the function

$$f : f(x) = \begin{cases} 1 & \text{if } x \text{ is in a long interval} \\ -1 & \text{if } x \text{ is in a short interval,} \end{cases} \quad (42)$$

which is local, but only piecewise continuous with breaks wherever x switches from a long to a short interval.

Graphs of these functions are shown (solid lines) in Figs. 7–11 and 12–15, respectively (see also Tables 1–4).

Our objective is to see how well the approximations we have discussed compare with the actual functions when the calculations are performed with specific choices of data points.

We approximate each of the two functions by a finite number of terms of its Fourier–Bohr expansion [equation (18)], which in our setting here reads

$$f(x) = \sum_{\tilde{k}\in\widetilde{\mathbb{Z}[\tau]}^\circ} a_k \exp\big(2\pi i(k \mid x)\big), \quad x \in \mathbb{R}. \quad (43)$$

For the two functions f chosen here, it is easy to determine the corresponding functions $\tilde{F}$ on the torus $\mathbb{T} = (\mathbb{R}\times\mathbb{R})/\widetilde{L}$ and hence to compute the Fourier–Bohr coefficients a_k exactly by equation (19) (see §6.2). For the nearest-neighbor function these are given explicitly in equation (50).

On the other hand, the approximation depends on the choice of the refinement lattice $\widetilde{L}_N$, which shall here always be of the form $(1/N)\widetilde{L} = (1/N)\widetilde{\mathbb{Z}[\tau]}$ (so the index $[\widetilde{L}_N : \widetilde{L}]$ is N^2). This determines both the points that will eventually be projected into our data points and also the values of k that shall be included in approximating the sum (43), namely a set $\widetilde{K}$ of $\widetilde{k} = (k, k') \in \widetilde{\mathbb{Z}[\tau]}^\circ$ chosen as representatives of the group $\widetilde{\mathbb{Z}[\tau]}^\circ/N\widetilde{\mathbb{Z}[\tau]}^\circ$ dual to the group $\big((1/N)\widetilde{\mathbb{Z}[\tau]}\big)/\widetilde{L}$. Our choice is to take $\widetilde{k}$ with $|k|$ as small as possible, so K consists of elements $k \in \mathbb{Z}[\tau]$, one for each congruence class of $\mathbb{Z}[\tau]$ modulo $N\mathbb{Z}[\tau]$, chosen so that $|k|$ is minimal in its class. We denote by $f^{\mathrm{exact}}(x)$ the finite series, taken from equation (43), approximating $f(x)$, $x \in \mathbb{R}$:

$$f^{\mathrm{exact}}(x) = \sum_{k\in K} a_k \exp\big(2\pi i(k \mid x)\big), \quad x \in \mathbb{R}. \quad (44)$$

Next we replace the coefficients a_k in $f^{\mathrm{exact}}(x)$ by their approximations

$$a_k^{\mathrm{int}} := (1/R)\int_0^R f(x)\exp\big(-2\pi i(k \mid x)\big)\,\mathrm{d}x \quad (45)$$

following from equation (22), and denote the resulting function by $f^{\mathrm{int}}(x)$. We shall use various values of R, all of which

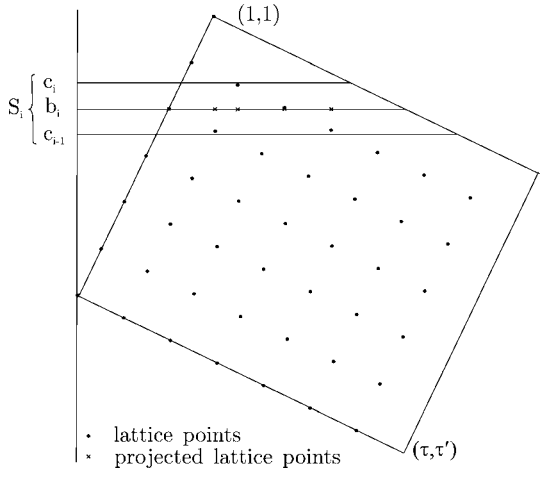

Figure 6
The points $\widetilde{s}_j$ lying in the strip S_i formed by the window $[c_{i-1}, c_i)$ are projected onto the segment l_i of the path $\{(t, 0)_L : 0 \le t \le R\}$ producing data points u_j, shown here as small crosses.

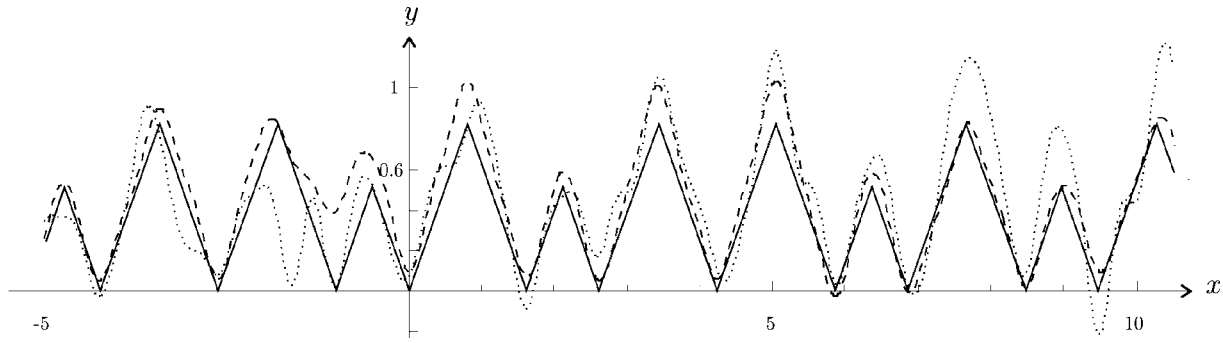

Figure 7
The solid line is the graph of f of equation (41). The dotted curve shows the $f^{\rm sum}$ approximation and the dashed curve shows the $f^{\rm int}$ approximation. Both approximations were calculated using a total of $N^2 = 49$ lattice points in C and $M = 11$ path passes in C, corresponding to an interval of integration $R \simeq 23, 30$. See §6.3 for an explanation of the misfit of approximations in the region $[-\tau^2, 0]$.

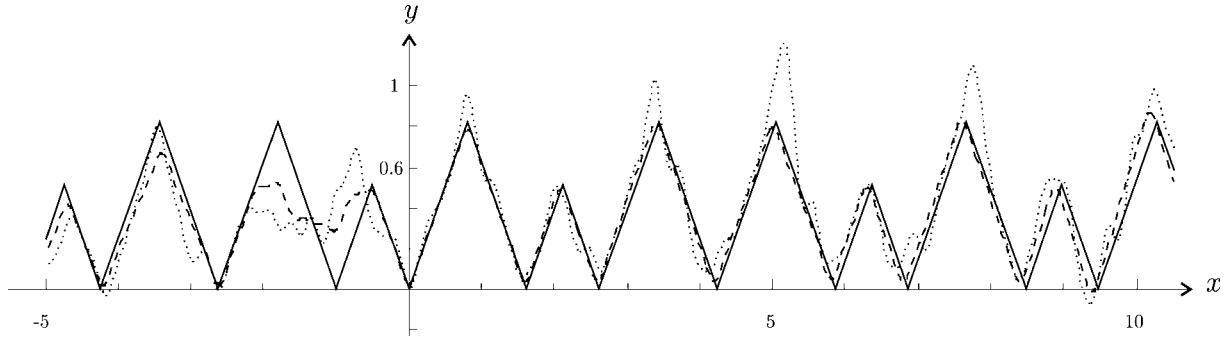

Figure 8
The function f and approximants of equation (41) are drawn with the same conventions as in Fig. 7, but for refined parameters $M = 17$, $N^2 = 121$ and $R \simeq 37, 43$.

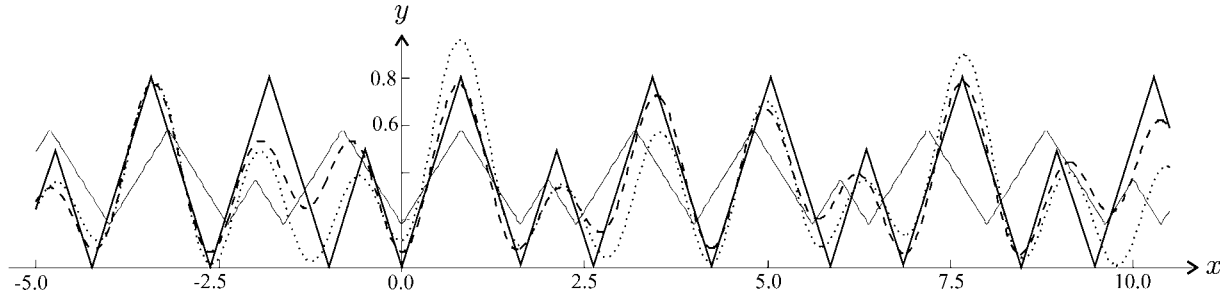

Figure 9
The function f of equation (41) is plotted for parameters $N^2 = 9$ lattice points from C, $M = 10$ passes of the fundamental domain and the corresponding interval of integration given by $R \simeq 21, 64$. The periodic approximation $f^{\rm cos}$ is shown. The number of cosine terms used is $n = 50$ and coefficients are calculated by formula (48). Here the dotted curve corresponds to the $f^{\rm sum}$ approximation, the dashed curve corresponds to the $f^{\rm exact}$ approximation and the thin line represents the $f^{\rm cos}$ approximation.

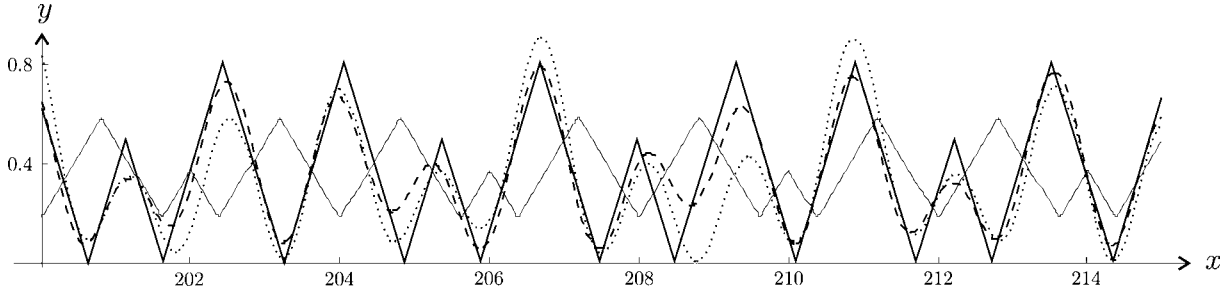

Figure 10
Here we plot the same approximations as in Fig. 9, but the functions are now drawn on the interval [200, 215]. Observe how the aperiodic approximants continue to follow the graph of f while the periodic approximant now has no relation to it.

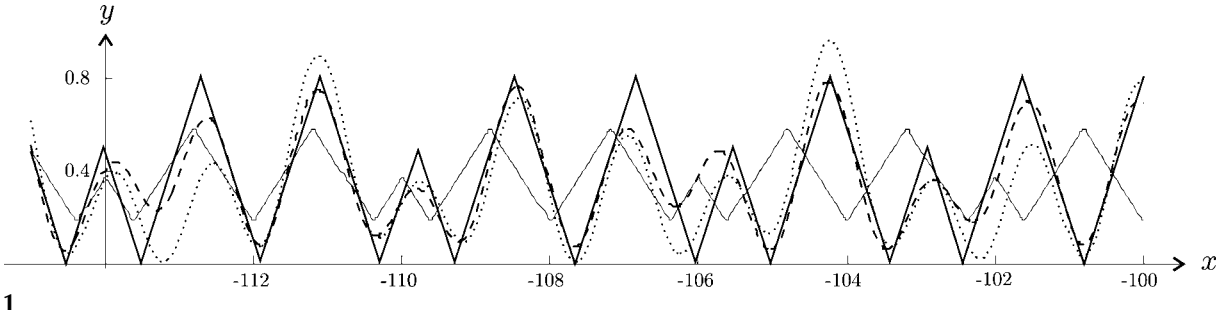

Figure 11
The approximations are presented with the same conventions as in Fig. 9 but the functions are drawn in the interval [−115, −100].

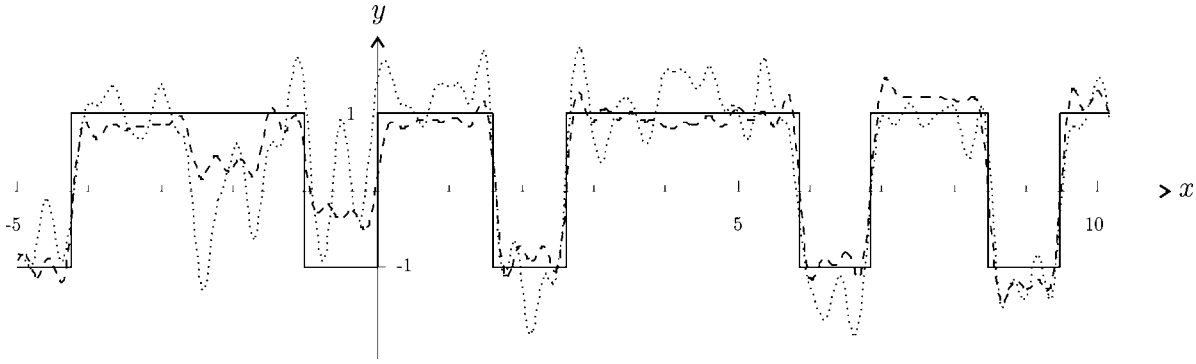

Figure 12
The solid line is the graph of f of equation (42). The dotted and dashed curves correspond to the $f^{\rm sum}$ and $f^{\rm int}$ approximations. Both approximations were calculated using a total of $N^2 = 81$ lattice points in C, $M = 17$ passes of C and the corresponding interval of integration given by $R \simeq 37,01$.

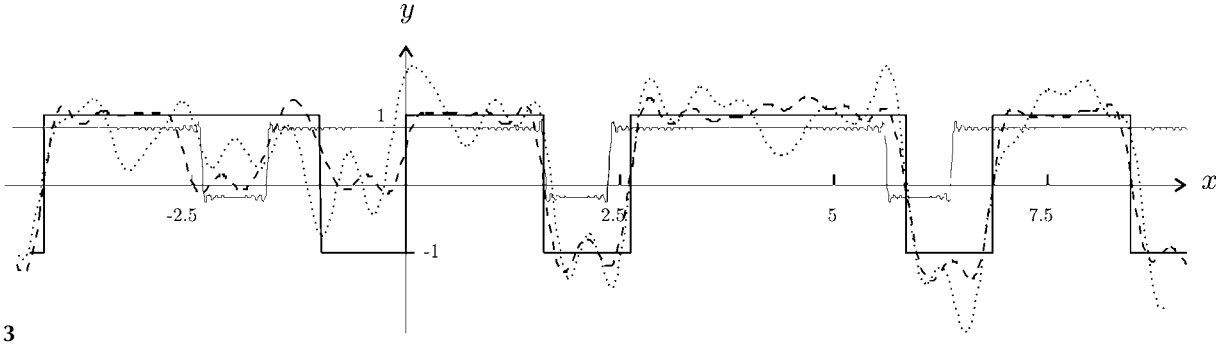

Figure 13
The function f of equation (42) is drawn for parameters: $N^2 = 49$, $M = 11$, $R \simeq 23,30$. The periodic approximation $f^{\rm cos}$ is also shown as a thin line. The number of cosine terms used is $n = 50$ and coefficients were calculated by equation (48). Here the dotted curve corresponds to the $f^{\rm sum}$ approximation and the dashed curve corresponds to the $f^{\rm exact}$ approximation.

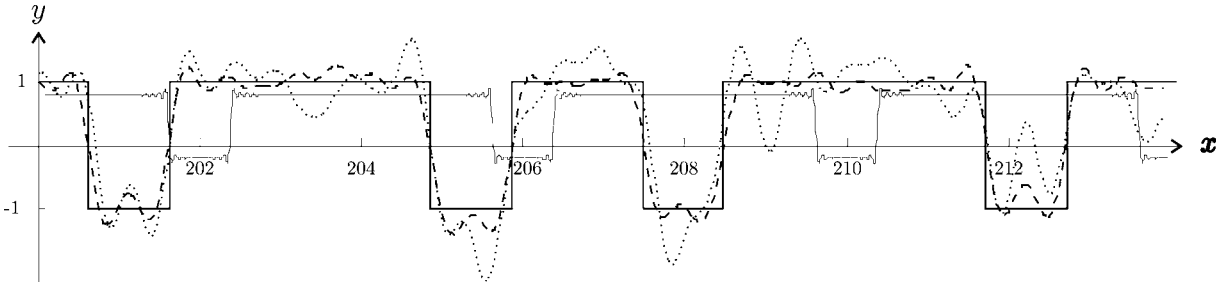

Figure 14
Here we adduce the same approximations as in Fig. 13, but the functions are drawn in the interval [200, 215].

Table 1
Comparison of the calculated coefficients a_k in the approximations f^{exact}, f^{int} and f^{sum} based on the parameters of Fig. 9.

k	a_k^{exact}	a_k^{int}	a_k^{sum}
$-\frac{1}{2}-\frac{1}{2}\tau$	$-0.1065 - 0.0367i$	$-0.1065 - 0.0371i$	$-0.1086 - 0.0581i$
$-\frac{1}{2}$	$0.0243 + 0.0287i$	$0.0236 + 0.0292i$	$0.0269 + 0.0711i$
$-\frac{1}{2}+\frac{1}{2}\tau$	$0.0026 + 0.0153i$	$0.0035 + 0.0155i$	$0.0233 - 0.0332i$
$-\frac{1}{2}\tau$	$-0.0683 + 0.0407i$	$-0.0680 + 0.0412i$	$-0.0517 + 0.0542i$
0	0.3618	0.3618	0.3367
$\frac{1}{2}\tau$	$-0.0683 - 0.0407i$	$-0.0680 - 0.0412i$	$-0.0517 - 0.0542i$
$\frac{1}{2}-\frac{1}{2}\tau$	$0.0026 - 0.0153i$	$0.0035 - 0.0155i$	$0.0233 + 0.0332i$
$\frac{1}{2}$	$0.0243 - 0.0287i$	$0.0236 - 0.0292i$	$0.0269 - 0.0711i$
$\frac{1}{2}+\frac{1}{2}\tau$	$-0.1065 + 0.0367i$	$-0.1065 + 0.0371i$	$-0.1086 + 0.0581i$

Table 2
Comparison of the values of the function f of equation (41) and its approximants f^{exact}, f^{int}, f^{sum} and $f^{\cos}$ (see Fig. 9).

x_i	$f(x_i)$	$f^{\text{exact}}(x_i)$	$f^{\text{int}}(x_i)$	$f^{\text{sum}}(x_i)$	$f^{\cos}(x_i)$
-100	0.8065	0.6916	0.6965	0.7728	0.1859
-50	0.4033	0.4229	0.4208	0.4562	0.3690
-15	0.3262	0.2555	0.2522	0.1461	0.4912
$-3-5\tau$	0	0.0577	0.0584	0.1378	0.5365
0	0	0.0658	0.0670	0.1165	0.1859
τ	0	0.0797	0.0788	0.0946	0.1858
$0.25+\tau$	0.2500	0.2060	0.2049	0.1995	0.3065
$0.5+\tau$	0.5000	0.3318	0.3313	0.3416	0.3138
$1+\tau$	0	0.1659	0.1649	0.1115	0.3000
$1+1.25\tau$	0.4045	0.3325	0.3287	0.1467	0.5022
$1+2.5\tau$	0.8090	0.6562	0.6609	0.6949	0.4681
$1+2.75\tau$	0.4045	0.3119	0.3152	0.2659	0.2659
50	0.4033	0.3265	0.3229	0.1209	0.3690
100	0.1885	0.3006	0.3004	0.2282	0.1859
500	0.4396	0.4669	0.4651	0.5364	0.1859

correspond to a set of complete passes across the fundamental region, as illustrated in Fig. 5.

The integrals (45) are to be estimated by reducing them to finite sums where the integrand is computed on the finite set of data arising as projections $\{u_1, \ldots, u_{N^2}\}$ of the N^2 points in C, as explained in §4.3:

$$a_k^{\text{sum}} := (1/N^2)\sum_{j=1}^{N^2} f(u_j)\exp\big(-2\pi i(k \mid u_j)\big). \tag{46}$$

The resulting approximation to $f^{\text{exact}}(x)$ is denoted $f^{\text{sum}}(x)$. This is the approximation that we have been working towards. Written out in full it reads

$$f^{\text{sum}}(x) = \sum_{k\in K}\Big\{(1/N^2)\sum_{j=1}^{N^2} f(u_j)\exp\big(-2\pi i(k \mid u_j)\big)\Big\}\exp\big(2\pi i(k \mid x)\big). \tag{47}$$

It is computed out of data points in $\mathbb{R}$, is a finite sum of exponential functions whose frequencies come from the Fourier module of f, and utilizes discrete groups arising out of the periodic setting of the underlying cut-and-project scheme. By its form, f^{sum} is almost periodic and approximates the function $\widetilde{F}$ everywhere on the real line as it lies wrapped around the torus.

Thus we have four functions: f, f^{exact}, f^{int} and f^{sum}, all defined for all $x \in \mathbb{R}$. The three approximation functions depend on the number M of passes of the real line going through the fundamental region C (see §§5.4 and 5.5 for details), and on the number N^2 of lattice points of $\widetilde{L}_N$ found in C. Each of them restricts the full summation of the Fourier–Bohr expansion to the same finite set K of frequencies. They differ because of the ways in which the Fourier–Bohr coefficients are obtained: they are exact in the first case (or at least as exact as real computation on computers can be), are derived from the integral approximation in the second, and come from the finite sum approximation to the integral in the third. The calculations and graphs shown in Figs. 7–15 allow one to compare these functions. The exact coefficients and their approximations by integrals are sufficiently close as to make little difference to the graphs, so the figures are restricted to comparing f, f^{int} and f^{sum}.

By way of comparison, there is one further Fourier approximant of the type that we obtain by periodically extending f from its values on a fixed finite interval I of $\mathbb{R}$ to the entire space $\mathbb{R}$. Thus we introduce

$$\begin{aligned} f^{\cos}(x) &= \sum_{k=0}^{n} a_k \cos(k\pi x/2), \quad \text{where} \\ a_k &= (1/2)\int_0^2 f(x)\cos(k\pi x/2)\,\mathrm{d}x. \end{aligned} \tag{48}$$

Needless to say, $f^{\cos}$ cannot be expected to have much relationship to f outside I, and it does not. In fact, $f^{\cos}$ does not appear to be a good choice even on the limited domain I.

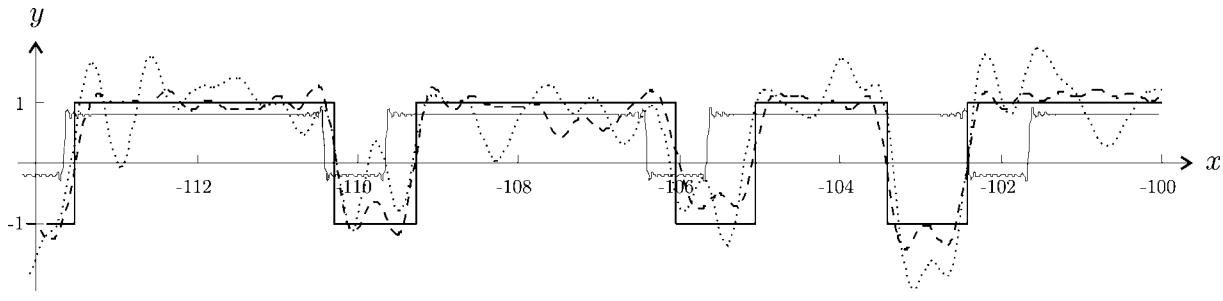

Figure 15
The approximations are drawn with the same conventions as on Fig. 13, but in the interval $[-115, -100]$.

Table 3
Comparison of the calculated coefficients a_k in the approximations $f^{\rm exact}$, $f^{\rm int}$ and $f^{\rm sum}$ based on the parameters $N^2 = 9$ and $M = 10$.

k	$a_k^{\rm exact}$	$a_k^{\rm int}$	$a_k^{\rm sum}$
$-\frac{1}{2}-\frac{1}{2}\tau$	0.1930 + 0.0094i	0.0228 + 0.0079i	0.1672 + 0.0576i
$-\frac{1}{2}$	0.2217 + 0.4063i	0.02971 + 0.0360i	0.2204 + 0.2603i
$-\frac{1}{2}+\frac{1}{2}\tau$	−0.0660 + 0.1738i	0.00384 + 0.0243i	0.0292 + 0.1744i
$-\frac{1}{2}\tau$	−0.1041 + 0.2138i	−0.0399 + 0.0240i	−0.2931 + 0.1744i
0	0.5556	0.0608	0.4472
$\frac{1}{2}\tau$	−0.1041 − 0.2138i	−0.0399 − 0.0240i	−0.2931 − 0.1744i
$\frac{1}{2}-\frac{1}{2}\tau$	−0.0660 − 0.1738i	0.0038 − 0.0243i	0.0292 − 0.1744i
$\frac{1}{2}$	0.2217 − 0.4063i	0.0297 − 0.0360i	0.2204 − 0.2603i
$\frac{1}{2}+\frac{1}{2}\tau$	0.1903 − 0.0094i	0.0228 − 0.0079i	0.1672 − 0.0576i

Table 4
Comparison of the values of the function f of equation (42) and its approximants $f^{\rm exact}$, $f^{\rm int}$, $f^{\rm sum}$ and $f^{\rm cos}$.

x_i	$f(x_i)$	$f^{\rm exact}(x_i)$	$f^{\rm int}(x_i)$	$f^{\rm sum}(x_i)$	$f^{\rm cos}(x_i)$
−100	1	1.0960	1.0796	1.1907	0.8024
−50	1	1.0690	1.0628	0.6269	−0.1948
−15	1	1.1020	1.1637	1.1570	0.8162
$-3-5\tau$	1	0.1092	0.0963	0.3515	0.8093
0	1	0.5331	0.5268	1.5952	0.8024
τ	−1	−0.0271	−0.0291	0.7757	0.3036
$0.25+\tau$	−1	−1.2750	−1.2957	−1.3115	−0.1820
$0.5+\tau$	−1	−0.7919	−0.8123	−0.7404	−0.1884
$1+\tau$	1	0.0704	0.0971	−0.0128	0.7910
$1+1.25\tau$	1	0.9261	0.9625	1.1215	0.8005
$1+2.5\tau$	1	1.1233	1.1382	1.0246	0.7991
$1+2.75\tau$	1	0.9577	0.9519	1.2470	0.7826
50	1	0.9241	0.9374	1.1735	−0.1948
100	−1	−1.2440	−1.2652	−1.5375	0.8024
500	1	1.0950	1.0639	0.9970	0.8024

6.2. Computing the exact Fourier–Bohr coefficients

It may be of interest to indicate how we computed the exact Fourier–Bohr coefficients. We can reorganize Fig. 3, translating the a and b regions into single blocks (Fig. 16), a procedure that is familiar from the *Klotz* construction (see §7) often used in studying cut-and-project sets (Kramer, 1987).

It is then straightforward to understand the corresponding function $\widetilde{F}$ on the two-dimensional torus, *i.e.* a genuinely periodic function for which $f(t) = \widetilde{F}(t, 0)$ mod $\widetilde{\mathbb{Z}[\tau]}$.

Furthermore, it is easy to compute the 'exact' Fourier coefficients of $\widetilde{F}$. Let $\widetilde{k} = a\widetilde{\omega}_1 + b\widetilde{\omega}_2 \in \widetilde{\mathbb{Z}[\tau]}^\circ$, where $a, b \in \mathbb{Z}$. Then

$$\big(\widetilde{k} \mid (x, y)\big) = x\big(\widetilde{k} \mid (1, 0)\big) + y\big(\widetilde{k} \mid (0, 1)\big) = 2xk\delta + 2yk'\delta',$$

where

$$k = (a + b\tau)/2, \quad k' = (a + b\tau')/2.$$

The Fourier coefficient for $\widetilde{k}$ is

$$a_k = \int_{\mathbb{T}} \widetilde{F}(w) \exp\big(-2\pi i(\widetilde{k} \mid w)\big)\, {\rm d}w = \int_0^1\int_0^1 \widetilde{F}(u, v) \exp\big(-2\pi i(\widetilde{k} \mid u\widetilde{1} + v\widetilde{\tau})\big)\, {\rm d}u\, {\rm d}v. \quad (49)$$

Writing

$$u\widetilde{1} + v\widetilde{\tau} = (u + v\tau, u + v\tau') =: (x, y),$$

we have

$$(\widetilde{k} \mid u\widetilde{1} + v\widetilde{\tau}) = 2kx\delta + 2k'y\delta'.$$

Making the change from the variables u and v to x and y, and using the definition of $\widetilde{F}$, we obtain

$$a_k = \frac{1}{\sqrt{5}} \int_{-1/\tau}^{0}\int_{-1}^{0} \left(\frac{1}{2} - \left|x + \frac{1}{2}\right|\right) \exp\big(-4\pi i(kx\delta + k'y\delta')\big)\, {\rm d}x\, {\rm d}y + \frac{1}{\sqrt{5}} \int_{-1/\tau}^{1/\tau^2}\int_{0}^{\tau} \left(\frac{\tau}{2} - \left|x - \frac{\tau}{2}\right|\right) \exp\big(-4\pi i(kx\delta + k'y\delta')\big)\, {\rm d}x\, {\rm d}y. \quad (50)$$

Note that the factor $1/\sqrt{5}$ comes from $x = u + v\tau$, $y = u + v\tau'$.

$$\begin{vmatrix} 1 & \tau \\ 1 & \tau' \end{vmatrix} = \tau' - \tau = -\sqrt{5}.$$

6.3. Shadows of singularities

Inspection of the aperiodic approximations shows that they are remarkably faithful to the originals. However, there is apparently a strange fuzziness in the approximation in the interval $[-\tau^2, 0]$. The explanation for this is quite interesting and shows that the approximation method we use here is sensitive to subtle qualities of the aperiodicity.

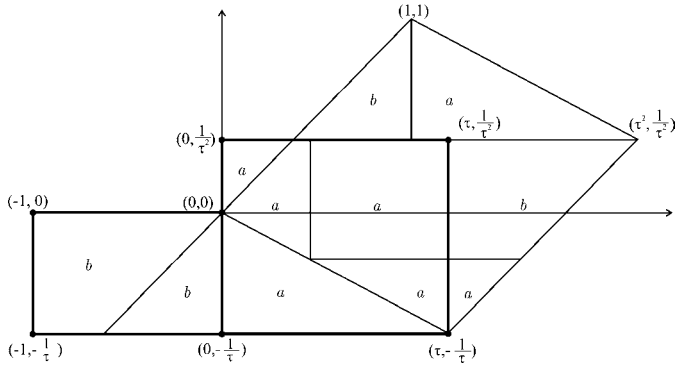

Figure 16
The a and b regions of Fig. 3 are reorganized here into two rectangles (heavy lines). The function $\widetilde{F}$ on $\mathbb{T}$ arising from the local function (41) is supported on these two rectangles. It is constant on vertical lines. Along the horizontal axis, on the b rectangle the function values start at 0, increase linearly to $\frac{1}{2}$ at the midpoint of the rectangle and then linearly decrease to 0 again. Similarly on the a rectangle they increase to $\tau/2$ and then return to 0.

The particular Fibonacci set that we have used in our example is singular, that is to say, it is one at which the torus parameterization is not 1–1. As pointed out in footnote 4, Λ is but one of two distinct sets in $X(\Lambda)$ that map to the same point on the torus $\mathbb{T}$ under the torus map. The other differs from Λ only in that it contains $\{-\tau\}$ but not $\{-1\}$. The Fourier analysis takes place on $\mathbb{T}$ and treats these two sets equally. However, the nearest-neighbor functions of the two sets are different. This is a difference that is immaterial to $\widetilde{F}$, which our function $f^{\rm sum}$ is approximating, but which the original function F can see. What we see is the Fourier analysis hedging between the two scenarios.

Further refinements of the lattice will never improve the situation in this interval. However, if we had used an element of $X(\Lambda)$ at which the torus map was 1–1 [and this is the case with probabilistic certainty if one chooses randomly from $X(\Lambda)$] then this phenomenon would not occur and the approximation would be uniformly valid over the entire space. All one need do is to shift the window so that its end points do not lie in the set $\mathbb{Z}[\tau]$, *e.g.* $\frac{1}{2}+[-1, 1/\tau]$.

7. Final comments

We should point out that there is considerable scope for adapting the scenario sketched out here. It is possible to arrange things so that they are related to tilings. One elegant tiling method is the *Klotz* construction (Kramer, 1987; Kramer & Schlottmann, 1989). One begins with the decomposition into Voronoi cells of the lattice $\widetilde{L}$ in $\mathbb{R}^d \times \mathbb{R}^d$ and along with it the corresponding dual cell decomposition into Delone cells. For each pair of P, Q consisting of intersecting d-dimensional faces P and Q from a Voronoi cell and a Delone cell, respectively, we form the *Klotz* $P^{\|} \times Q^{\perp}$ in $\mathbb{R}^d \times \mathbb{R}^d$. The set of these *Klötze* form a tiling of $\mathbb{R}^d \times \mathbb{R}^d$. Furthermore, the intersection of $(\mathbb{R}^d, 0)$ with this tiling produces a tiling of physical space. (If one chooses instead to perform the projections the other way around, one gets a different tiling.) Several of these *Klötze* can be combined to form a fundamental region for $\mathbb{R}^d \times \mathbb{R}^d$, as we see in Fig. 16, and this type of choice should lead to computational methods that are adapted to these tilings. For instance, the region A of integration might well be chosen as the union of a finite number of tiles. For more on determining Voronoi and Delone cells in the context of high symmetry, see Moody & Patera (1995).

The method advocated here is based on the idea of local functions, the extension of them into the context of compact Abelian groups, and the discretization of the resulting Fourier analysis by the use of finite groups. In the one-dimensional setting that was explored in detail here, the only symmetries involved arise from translational symmetry (which is at the base of the almost periodicity). In higher dimensions, especially those of interest to the quasicrystal community, decagonal, icosahedral or other symmetries appear. In these cases there are a number of ways of utilizing the symmetry to greatly improve the efficiency of the computation, in the same spirit as Moody & Patera (1984). As we have pointed out, the preparations required for this depend largely on the cut-and-project scheme and not so much on the actual model set involved. Fortunately the cut-and-project schemes for these settings are essentially canonical and their strong algebraic nature makes this program quite feasible.

Finally, although we have not spelled it out here, the way in which finite groups and their duals are used here makes the process amenable to the technique of the fast Fourier transform. Details will appear later.

This work was supported in part by the Natural Sciences and Engineering Research Council of Canada, the MIND Research Institute of Santa Ana, California, the Aspen Center for Physics, and MITACS. The authors are grateful to the referees for their constructive comments.

References

Amerio, L. & Prouse, G. (1971). *Almost-Periodic Functions and Functional Equations*. New York: Litton Educational Publishing.
Besicovitch, A. S. (1954). *Almost Periodic Functions*. Cambridge: Dover Publications.
Bochner, S. (1927). *Proc. London Math. Soc.* **26**, 433–452.
Bochner, S. (1962). *Proc. Natl Acad. Sci. USA*, **48**, 195–205.
Bochner, S. & von Neumann, J. (1935). *Trans. Am. Math. Soc.* **37**, 21–50.
Bohl, P. (1893). *Über die Darstellung von Funktionen einer Variabeln durch trigonometrische Reihen mit mehreren einer Variabeln proportionalen Argumenten* (Thesis), University of Dorpat, Estonia.
Bohr, H. (1947). *Almost Periodic Functions*. Providence: American Mathematical Society/Chelsea Publishing Company.
Burckel, R. B. (1970). *Weakly Almost Periodic Functions on Semigroups*. New York: Gordon and Breach Science Publishers.
Chen, L., Moody, R. V. & Patera, J. (1998). *Quasicrystals and Discrete Geometry*, Fields Institute Monograph Series, Vol. 10, edited by J. Patera, pp. 135–178. Providence: American Mathematical Society.
Hof, A. (1995). *Commun. Math. Phys.* **169**, 25–43.
Keller, G. (1998). *Equilibrium States in Ergodic Theory*, LMS Student Texts, Vol. 42. Cambridge University Press.
Kramer, P. (1987). *Mod. Phys. Lett. B*, **1**, 7–18.
Kramer, P. & Schlottmann, M. (1989). *J. Phys. A*, **22**, L1097–L1102.
Levitan, B. M. & Zhikov, V. V. (1982). *Almost Periodic Functions and Diffferential Equations*. Cambridge University Press.
Meyer, Y. (1972). *Algebraic Numbers and Harmonic Analysis*. Amsterdam, London: North-Holland.
Moody, R. V. (1997). *Model Sets and Their Duals, The Mathematics of Long-Range Order*, NATO ASI Series, Vol. C489, edited by R. V. Moody, pp. 239–268. Dordrecht: Kluwer.
Moody, R. V. & Patera, J. (1984). *SIAM J. Algebraic Discrete Methods*, **5**, 359–383.
Moody, R. V. & Patera, J. (1995). *Can. J. Math.* **47**, 573–605.
Moody, R. V. & Patera, J. (2006). *SIGMA*, **2**, 076.
Radin, C. & Wolf, M. (1992). *Geometriae Dedicata*, **42**, 355–360.
Schlottmann, M. (2000). *Directions in Mathematical Quasicrystals*, CRM Monograph Series, Vol. 13, edited by M. Baake & R. Moody, pp. 143–159. Providence: American Mathematical Society.
Weyl, H. (1926–1927). *Math. Ann.* **97**, 473–498.
Wiener, N. (1926). *Math. Z.* **24**, 575–616.